ABSTRACT

Title of Document: EFFORTS TOWARD SYNTHESIS OF NOVEL ANALOGS OF THE BACTERIAL SECOND-MESSENGER, C-DI-GMP

Andrew J. Shurer, M.S., 2009

Directed By: Assistant Professor Herman O. Sintim, Department of Chemistry and Biochemistry

The formation of bacterial biofilms is a common mechanism for antibiotic resistance. It has been shown that bis-(3'-5')-cyclic dimeric guanosine monophosphate, c-di-GMP, plays a key role in bacterial biofilm formation; therefore, the proteins that regulate the metabolism or adaptive response of c-di-GMP are favorable targets for novel antimicrobials. We herein describe a solid-support methodology developed in the Sintim Laboratory and efforts toward its application to the synthesis of novel c-di-GMP analogs. Our selected targets are a series of analogs bearing various substitutions at the 2'-position of the ribose backbone. Syntheses of 2'-deoxy and 2'-methoxy analogs were achieved as well as that of key intermediates toward the 2'-fluoro and conformationally flexible analogs.

EFFORTS TOWARD SYNTHESIS OF NOVEL ANALOGS OF THE BACTERIAL-SECOND MESSENGER, C-DI-GMP

By

Andrew J. Shurer

Thesis submitted to the Faculty of the Graduate School of the
University of Maryland, College Park, in partial fulfillment
of the requirements for the degree of
Master of Science
2009

Advisory Committee:
Assistant Professor Herman O. Sintim, Chair
Assistant Professor Ashton Cropp
Professor Philip DeShong
Professor Steven Rokita

Acknowledgements

I would like to thank Dr. Julie Ray, formally of the University of Maryland, Baltimore School of Pharmacy Mass Spectrometry Facility and Dr. Philip Mortimer of the Johns Hopkins University Mass Spectrometry and Proteomics Facility for mass spectral data. I would also like to thank Dr. Sintim and current and former members of the Sintim Laboratory for helpful discussions.

Table of Contents

List of Tables

List of Figures

List of Schemes

List of Abbreviations

CPG	controlled-pore glass
DGC	diguanylate cyclases
DHPG	1,3-dihydroxy-2-propoxymethyl guanine
DMF	N', N'-dimethylformamidine
DMSO	dimethylsulfoxide
DMT	dimethoxytrityl
DNA	deoxyribonucleic acid
DNAse	deoxyribonuclease
ESI-MS	electrospray ionization – mass spectrometry
G	guanine
GTP	guanosine triphosphate
h	hours
HMPA	hexamethylphosphoramide
HPLC	high performance liquid chromatography
^{i}Bu	isobutyryl
IMP	imidazolium perchlorate
Me	methyl
min	minutes
MS	molecular sieves
MSNT	1-(mesitylene-2-sulfonyl)-3-nitro-1,2,4-triazole
NMR	nuclear magnetic resonance
OAc	Acetate
PDE	phosphodiesterase
RNA	ribonucleic acid
RNAse	ribonuclease
s	seconds
TBS	tertbutyldimethylsilyl
TLC	thin-layer chromatography
TPSCl	triisopropylbenzenesulfonyl chloride
TRIS	tris(hydroxymethyl)aminomethane
U	uridine

Chapter 1: Introduction

1.1 The Rise of Antibacterial Resistance

With the rise of antibiotics in the 1940's through 1960's, the treatment of infectious diseases had greatly increased the quality of life and lengthened life expectancy.[1] In 1969, Surgeon General William H. Stewart[2] addressed the United States' Congress saying that it was time to 'close the book on infectious diseases'. Today, however, infectious disease is prevalent. In 1998, infectious diseases accounted for 13.3 million deaths world-wide.[3] The resurgence of infectious diseases could be attributed to the rise of antibacterial resistance.[13]

According to the United States Food and Drug Administration, about 70 percent of infection-causing bacteria in hospitals are resistant to at least one of the drugs most commonly used to treat such infections.[4] Table 1[5] illustrates the prevalence of resistance in hospital-acquired infections as of 2004.

Table 1. Prevalence of resistance in hospital-acquired infections, US 2004[5]

Antibiotic	Pathogen	Resistance [%]
methicillin	*S. aureus*	59.5
	coagulase-negative staphylococci	89.1
vancomycin	enterococci	28.5
cephalosporins	*Enterobacter* spp.	31.1
3rd generation	*P. aeruginosa*	31.9
	E. coli	5.80
	K. pneumoniae	20.6
imipenem	*P. aeruginosa*	21.4
quinolones	*P. aeruginosa*	29.5

Furthermore, in the 1980s, pharmaceutical companies began reducing the development of new antibiotics.[6,7] We can no longer rely on pharmaceutical companies to provide the next generation antibiotics in a timely fashion. As a result, academic scientists have embarked on the search for potential antibiotics with novel modes of action. One pathway for antibiotic development currently under investigation by the academic community is cell-to-cell communication, or quorum sensing, as it pertains to the formation of bacterial biofilms.[8]

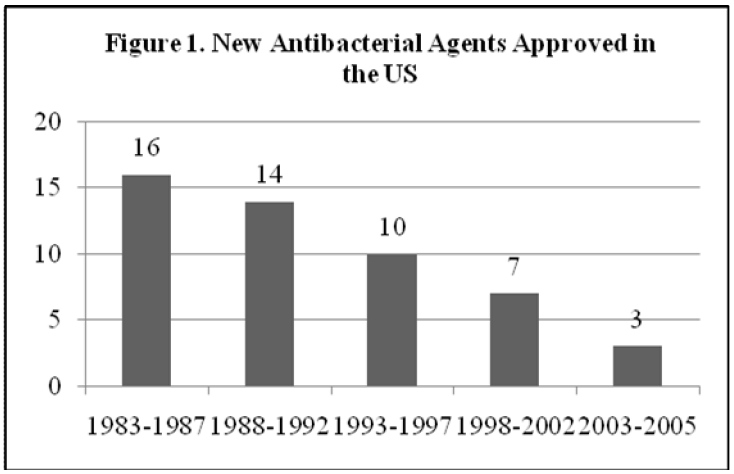

Figure 1. New antibacterial agents approved in the US.[5]

1.2 Bacterial Biofilms

The definition of a biofilm has evolved over the years. The currently accepted definition is as follows: 'a microbially derived sessile community characterized by cells that are irreversibly attached to a substratum or interface or to each other, are embedded in a matrix of extracellular polymeric substances that they have produced, and exhibit an altered phenotype with respect to growth rate and gene transcription.'[8] Put simply, biofilms are a community of bacteria that are protected by an extracellular

matrix. In the biofilm environment, bacteria are able to survive harsh environmental conditions. Bacterial biofilms have been observed and studied for decades, yet are far from being well-understood. For example, it is known that biofilms are involved in antibacterial resistance. However, currently, the mechanism of this resistance is not known, though several hypotheses have been formulated to account for how the formation of biofilms leads to antibiotic resistance.[8]

It has been argued that in the biofilm environment, there are more opportunities for gene-transfer between bacteria, thus leading to resistance.[9,10,11] However, this does not account for resistance that is observed in bacteria that lack a resistance gene. It is plausible then that the path to resistance arises from the physical barrier created by the formation of a biofilm.[12,13,14] This protective barrier, which is formed by the extracellular matrix, is not easily crossed by conventional antibiotics, and thus, resistance can develop.[15] It is likely that the rise of bacterial resistance to conventional antibiotics when in the biofilm environment is due to the combined effect of these factors.

The discovery of small molecules to regulate biofilm formation may have utility in the treatment of bacterial infections. When used in concert with a biofilm inhibitor, current antibiotics may once again be rendered effective. However, as already discussed, little is known in the area of bacterial biofilms. If synthetic small molecules are to play a role in modulating biofilm formation, the key processes that govern the onset or maturation of bacterial biofilms must be fully understood.

Bacterial communication plays a major role in facilitating biofilm formation and is therefore an area of intensive investigation by several groups worldwide.[16]

1.3 c-di-GMP, a Ubiquitous Bacterial Second-Messenger

In recent years it has been shown that bis-(3'-5')-cyclic dimeric guanosine monophosphate, c-di-GMP (Figure 2), plays a key role in bacterial biofilm formation.[17]

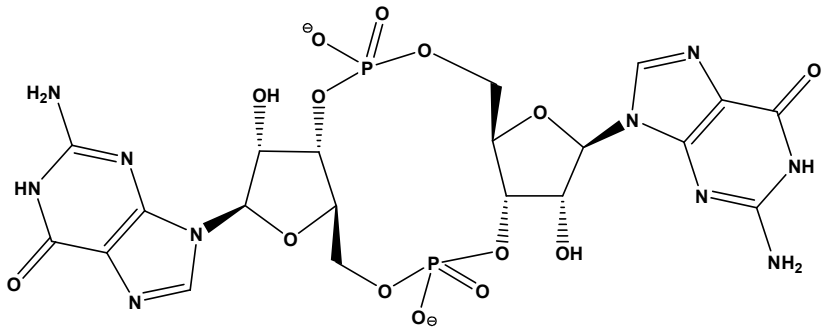

Figure 2. Bis-(3'-5')-cyclic dimeric guanosine monophosphate, c-di-GMP.

First described by Benziman *et. al.* as a regulator of cellulose synthase in *Gluconacetobacter xylinus,*[18] c-di-GMP is now described as an almost ubiquitous bacterial second-messenger.[17] Second-messengers are small molecules whose role is to link specific environmental cues to a particular response. This is generally achieved by changes in the intracellular concentration of the second-messenger in response to environmental cues. The use of second-messengers has several advantages. For example, the generation of the second-messenger may lead to

amplification of a signal. Also, second-messengers are often able to diffuse throughout the cell and affect other processes.[19]

C-di-GMP is known to be involved in a large number of functions in bacteria which include, but are not limited to the following: developmental transitions,[20] aggregative behavior and adhesion (e.g. biofilm formation),[21,22] and virulence.[23] The central role that c-di-GMP plays in biofilm formation makes the proteins or other macromolecules involved in regulating the metabolism or adaptive response of c-di-GMP favorable targets for novel antimicrobials. This highlights the need to gain insight into the metabolism of c-di-GMP in the cell (Figure 3).

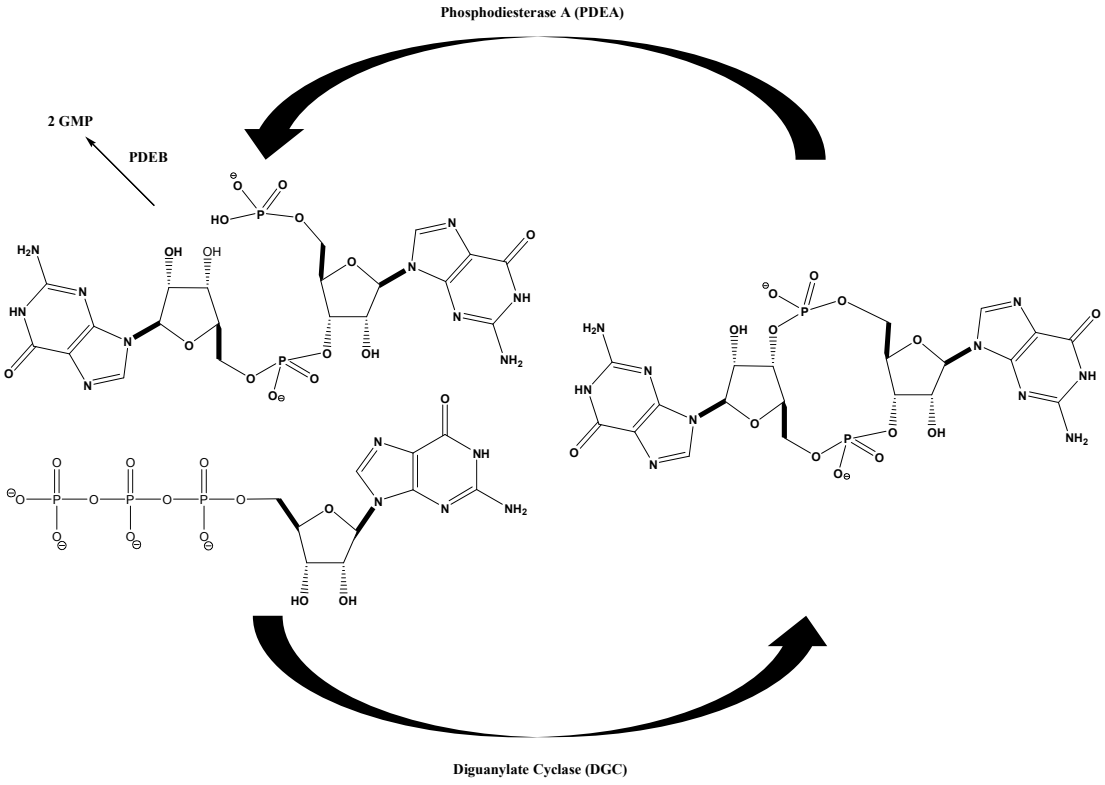

Figure 3. Metabolism of c-di-GMP.

Currently it is known that a family of proteins known as diguanylate cyclases (DGC's), which contain the common protein domain GGDEF (glycine-glycine-aspartate-glutamate-phenylalanine), synthesize c-di-GMP from GTP. The structure of a DGC from PleD, a regulatory protein from *Caulobacter crescentus* has been elucidated *via* X-ray crystallography.[24] In this seminal work, Jenal *et. al.* have shown that the majority of DGC's have an allosteric inhibition site that binds to dimeric c-di-GMP in the crystalline state. In other words, c-di-GMP regulates its synthesis by negative feedback.

A little understood family of proteins known as phosphodiesterases (PDE's), characterized by the EAL (glutamate-alanine-leucine) protein domain, is responsible for degradation of c-di-GMP.[25,20] This domain was first described as a modulator of c-di-GMP by Benziman *et. al.* through studies of the regulation of cellulose synthesis in *G. xylinus*,[18] It was later described by Merkel *et. al.* in *BvgR* as a repressor of virulence gene expression in *Bordetella pertussis.*[26] Over-expression of genes coding for EAL domain-containing proteins lead to reduced c-di-GMP levels in the cell, suggesting a role in c-di-GMP degradation.[27,28,29] Conversely, it was shown that mutating the EAL domain leads to an increase in the concentration of c-di-GMP.[30] However, the exact enzymatic mechanism of c-di-GMP degradation is unknown.

In addition to its wildly diverse set of biological functions, c-di-GMP also displays an array of interesting structural characteristics. For example, in 1990, Wang illustrated

by X-ray crystallography that c-di-GMP adopts an intercalated quartet organization, with four guanines stacked on one another (Figure 4).[31,32]

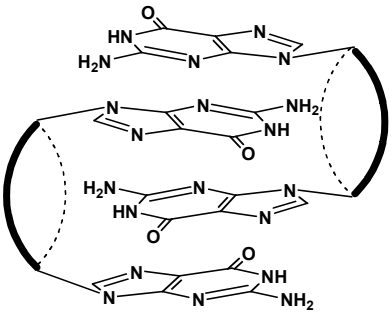

Figure 4. Intercalated quartet form of c-di-GMP.

While crystal structures can be valuable tools in confirming the structure of a compound, ultimately, solution phase structures can be more useful in understanding how molecules interact with various proteins and other small molecules.

Recently, Jones *et. al.* have shown that in solution phase, high concentrations of c-di-GMP can also exist in an intercalated dimeric form. Using a well-designed series of ultraviolet spectroscopy, circular dichroism, and one and two-dimensional nuclear magnetic resonance experiments, Jones has illustrated the metal-ion dependent polymorphism of c-di-GMP.[33,34] This work shows that c-di-GMP can adopt an array of various structures in solution, in response to the presence of different metals. However, Jones' work raises several questions which will be discussed later.

1.4 Evolution: The Synthesis of c-di-GMP

The ability to use chemical probes to study this important bacterial signaling system is limited by access to the molecule of interest and its analogs. The synthesis of c-di-GMP has proven challenging for chemists in this field since the earliest indication of its importance. Enzymatic synthesis provides a rapid route to c-di-GMP from GTP. However, the enzymatic synthesis of c-di-GMP analogs is non-trivial since enzymes usually have substrate specificity. A chemical synthesis is desirable for obtaining analogs in the quantity that will be necessary for the types of in-depth studies that will be required to fully elucidate the complexities of this system. The chemical synthesis of c-di-GMP has evolved over time. There are currently both solution phase and solid support routes to this compound.

The first chemical synthesis of c-di-GMP was reported by van Boom *et. al.* in the late 1980's (Scheme 1).[35] This method employed a phosphotriester approach to natural and unnatural cyclic oligonucleotides. This approach, developed in collaboration with Benziman *et. al., g*ave access to these compounds in order to make observations into the processes of cellulose synthase, which is regulated by c-di-GMP.

Unfortunately, detailed experimental conditions never accompanied this work. When the link was made between c-di-GMP and biofilm formation, several groups began exploring new approaches to making these compounds.

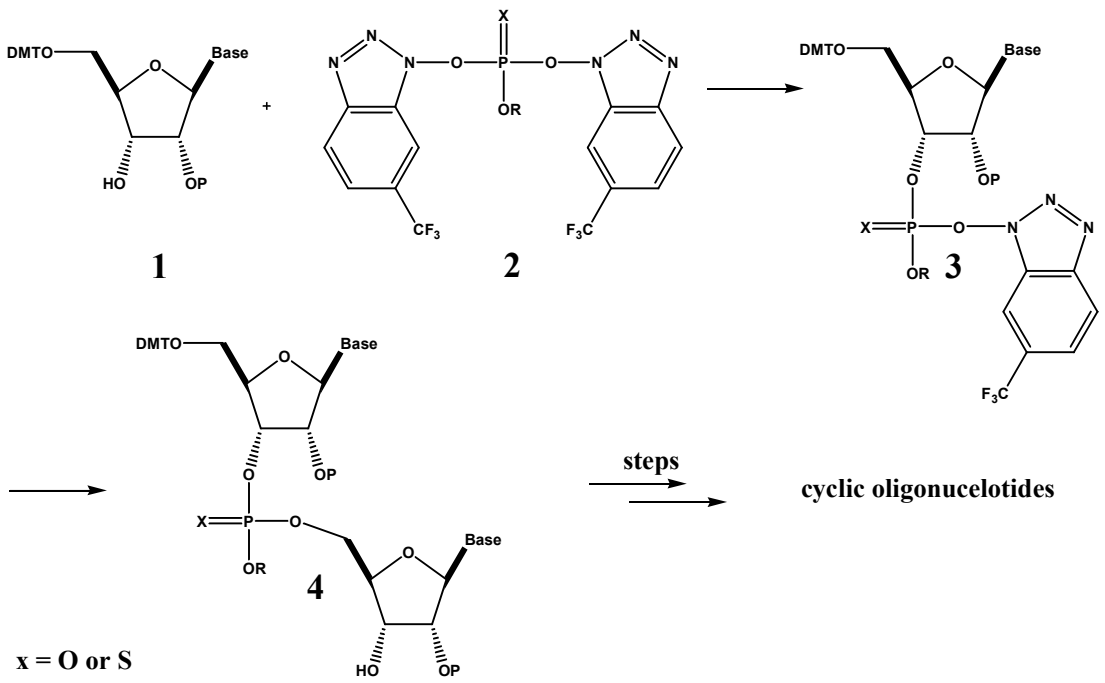

Scheme 1. Van Boom's phosphotriester approach to cyclic oligonucleotides.

In 2003, Hayakawa reported a phosphoramidite coupling approach to synthesize c-di-GMP (Scheme 2).[36] Hayakawa'a approach begins with commercially available phosphoramidites **5**. Oxidation of compound **5** with 2-butanone peroxide followed by deprotection of the dimethoxytrityl (DMT) group affords phosphate **6**. Next, the two building blocks (phosphate **6** and phosphoramidites) are coupled in the presence of imidazolium perchlorate (IMP) in acetonitrile to give **7**. A subsequent oxidation followed by deprotection of the allyl group and cyclization with a mixture of triisopropylbenzenesulfonyl chloride (TPSCl) and N-methylimidazole in tetrahydrofuran yields the cyclic oligonucleotide **8**. Compound **9** is then converted into c-di-GMP by standard deprotection protocols.[37]

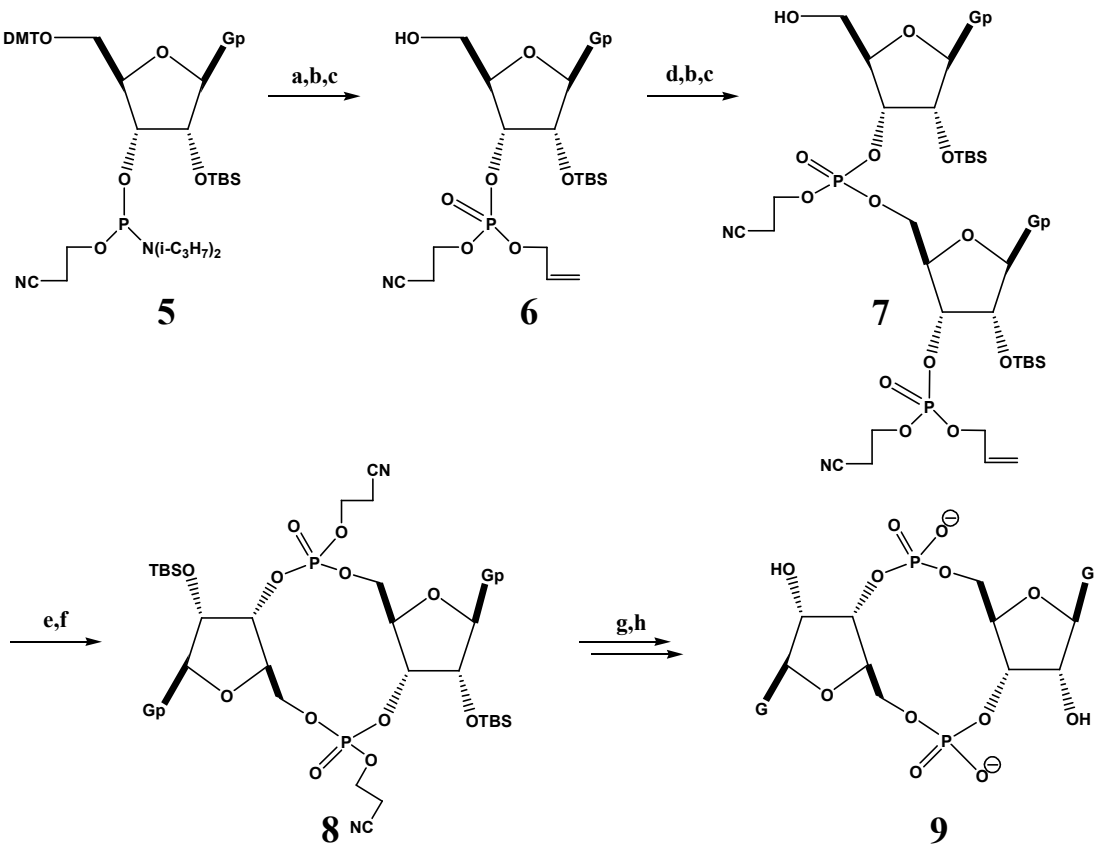

Gp = N^2-(allyloxycarbonyl)-O^6-(allyl)guanine

Scheme 2. Hayakawa's synthesis of cGpGp. (a) 2-cyanoethanol, imidazolium perchlorate, MS 3A, CH_3CN; (b) 6.7% 2-butanone peroxide/toluene solution; (c) dichloroacetic acid, CH_2Cl_2, 0 ^oC; (d) phosphoramidite **5**, imidazolium perchlorate, MS 3A, CH_3CN; (e) concentrated aqueous ammonia:CH_3OH (1:10 v/v); (f) triisopropylbenzenesulfonyl chloride, N-methylimidazole, tetrahydrofuran; (g) Pd_2(dibenzylideneacetone)$_3$, $CHCl_3$, triphenylphosphine, butylammonium formate, tetrahydrofuran; (h) triethylamine trihydrofluoride.

Hayakawa's method provided a synthesis of c-di-GMP and its analogs. However, this method involves several steps and tedious column chromatographic separations. To make c-di-GMP analogs readily available, a better synthetic strategy was required.

In 2004, Roger Jones *et. al.* reported a new solution phase approach to c-di-GMP using an H-phosphonate cyclization as the key step.[28] In this method (Scheme 3) the

H-phosphonate group serves as a protecting group during the coupling step. However, the length of the overall procedure is not reduced.

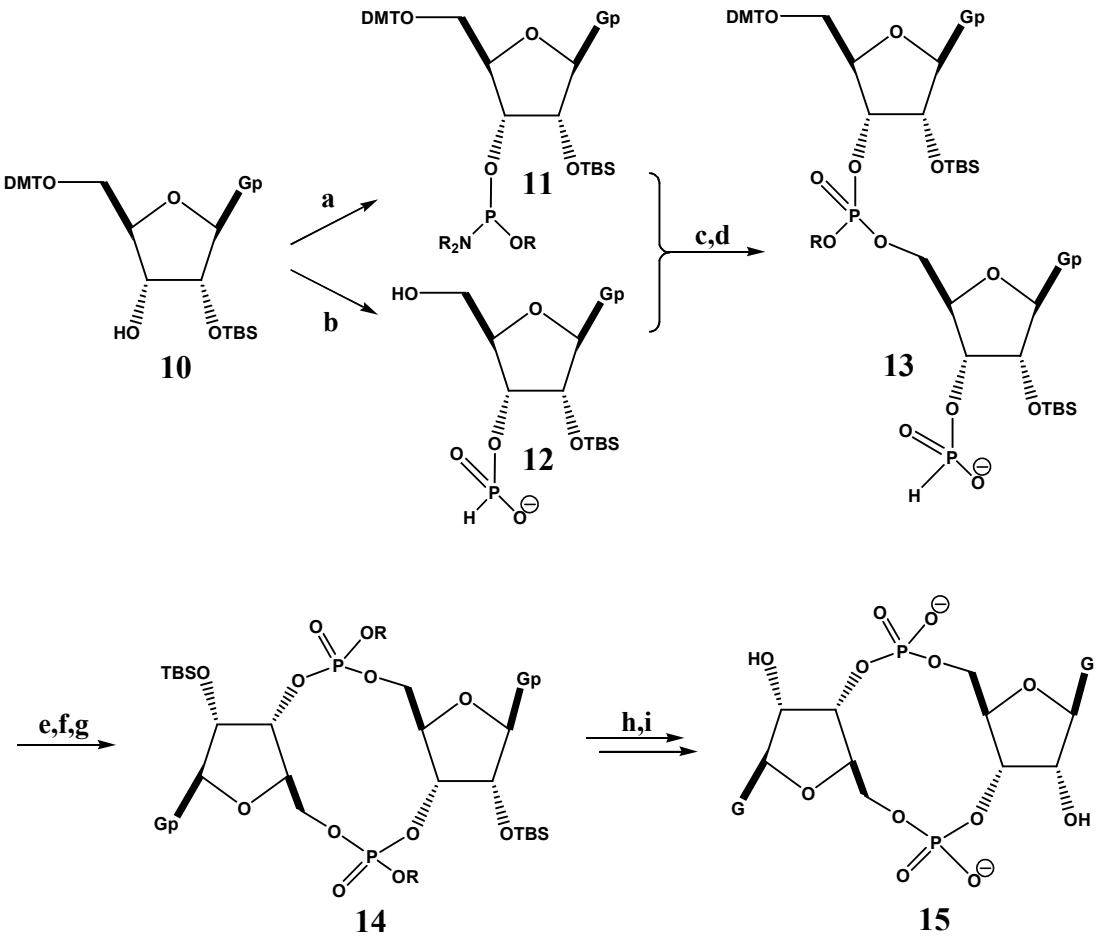

Scheme 3. Jones' phosphotriester, H-phosphonate method. (a) Bis(diisopropylamino)methyl or bis(diisopropylamino)cyanoethyl phosphoramidite and pyridinium trifluoroacetate; (b) 2-chloro-4H-1,3,2-benzodioxaphosphorin-4-one; (c) pyridinium trifluoroacetate; (d) *tert*-butylhydroperoxide; (e) sulfonic acid resin; (f) adamantoylcarbonyl chloride; (g) CH_3OH/N-bromosuccinimide; (h) pyridine/aqueous ammonia (1:1); (i) triethylamine trihydrofluoride.

Currently, there are also several solid-support approaches to the synthesis of these compounds. Solid-support chemistry provides several advantages over traditional solution phase chemistry. Immobilizing the molecule onto a resin allows for use of

large excesses of reagent to push the reaction to completion. Also, these methods eliminate the need for exhaustive purification of intermediates by allowing excess reagents and by-products to be removed by filtration and successive washings. Solid-support methods also create the opportunity for large portions of the synthesis to be carried out on an automated DNA synthesizer.

The first reported solid-support approach to cyclic oligonucleotides was reported in 1993.[38,39] In this method, the exocyclic amino group of cytosine is attached to the solid support, where elongation and cyclization are then carried out. This method is of course limited by the fact that cytosine must be present in the sequence.

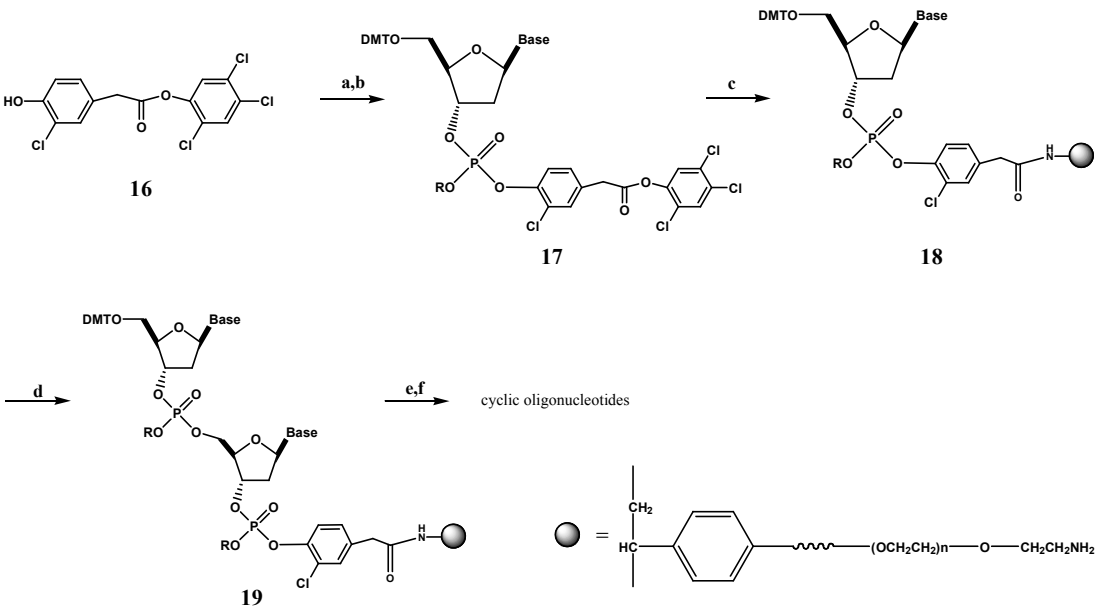

Scheme 4. Pedroso's solid-support approach to cyclic oligonucleotides. (a) phosphoramidite, tetrazole; (b) iodine/pyridine; (c) Tenta gel, N,N-dicyclohexylcarbodiimide, hydroxybenzotriazole; (d) trichloroacetic acid, phosphoramidite, tetrazole, followed by iodine/pyridine; (e) 1-(mesitylene-2-sulfonyl)-3-nitro-1,2,4-triazole; (f) tetramethylguanidinium *syn*-pyridine-2-aldoximate, concentrated aqueous ammonia.

The next reported method for solid-support synthesis of cyclic oligonucleotides was that of Pedroso in 1997.[40] Pedroso reported an elegant synthesis (Scheme 4) that circumvented the need for a particular base in the sequence. However, in Pedroso's method, two solution phase reactions are required before attaching the substrate to the solid support. This reduces some of the benefits of doing solid-phase synthesis. Perhaps more limiting, Pedroso's methodology is not amenable to RNA analogs bearing a bulky 2'-substituent. Additionally, this chemistry was not repeatable in our hands.

In 2002, Kool and co-workers published another synthesis of short cyclic oligonucleotides.[41] Although Kool did not make c-di-GMP, as the importance of this molecule was not known at the time, the method can be extended to the synthesis of c-di-GMP. Kool's approach (Scheme 5) utilizes an oxidative sulfurization with the commercial reagent 3H-1,2-benzodithiol-3-one-1,1-dioxide (Beaucage reagent) leading to the thiophosphotriester. After the second coupling cycle and removal of the terminal 5'-dimethoxytrityl group; iodination of the 5'-end is performed. Deprotection of bases, release from the CPG support, and cyclization by S_N2 displacement, are all conducted in a single step by treatment with concentrated ammonium hydroxide for 24 h at room temperature.

The obvious shortcoming to this method is that it forms cyclic oligodinucleotides with a sulfur atom replacing one of the bridging phosphodiester oxygen atoms. It

remains to be seen how this sulfur-for-oxygen replacement affects biological activities.

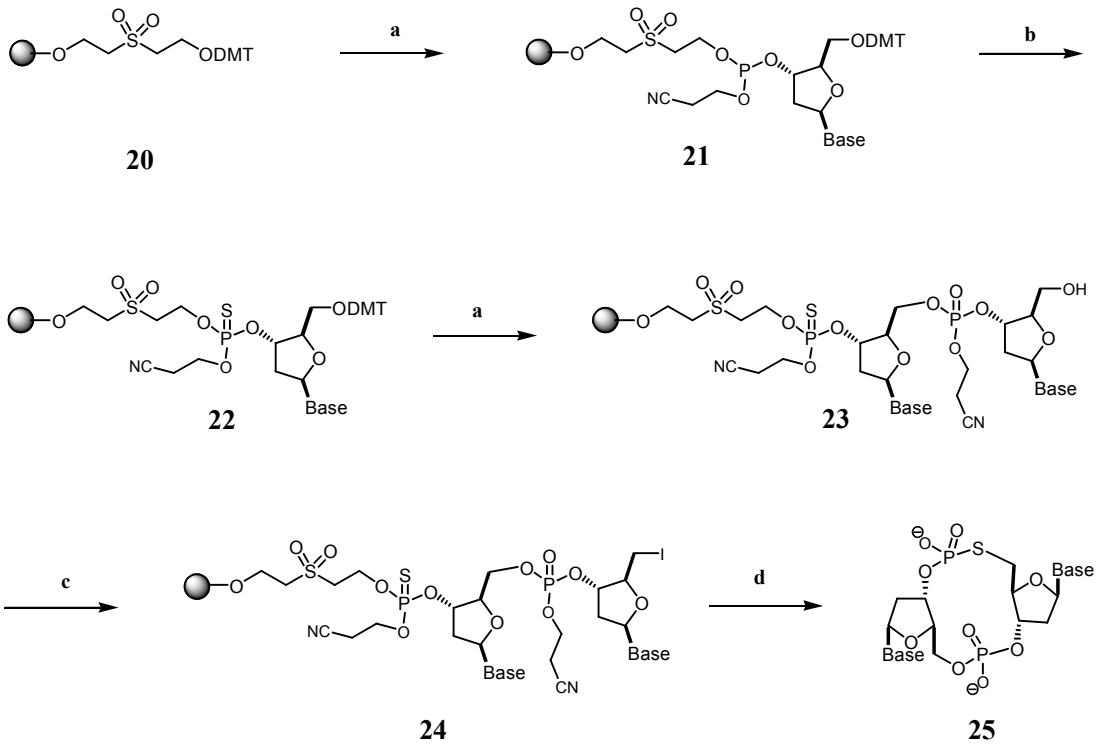

Scheme 5. Kool's synthesis of phosphothioates. (a) programmed synthesis on a DNA synthesizer; (b) 3H-1,2-benzodithiol-3-one-1,1-dioxide, CH_3CN; (c) $(PhO)_3PCH_3I$, dimethylformamide; (d) 28% aqueous ammonium hydroxide, RT, 24 h.

Our lab has developed a solid-phase methodology to access c-di-GMP and analogs that is without the aforementioned shortcomings.[42] In our method (Scheme 6) the protected dinucleotides on the CPG solid support are obtained on a DNA synthesizer. For this approach, the P-methoxy phosphoramidite is used for both coupling steps. Treatment of the solid-supported dinucleotide **26** with triethylamine, followed by 1-(mesitylene-2-sulfonyl)-3-nitro-1,2,4-triazole (MSNT), yields the cyclic dinucleotide

28. This approach consists of cleavage of the dinucleotide into solution followed by cyclization in the same pot without any isolation or purification.

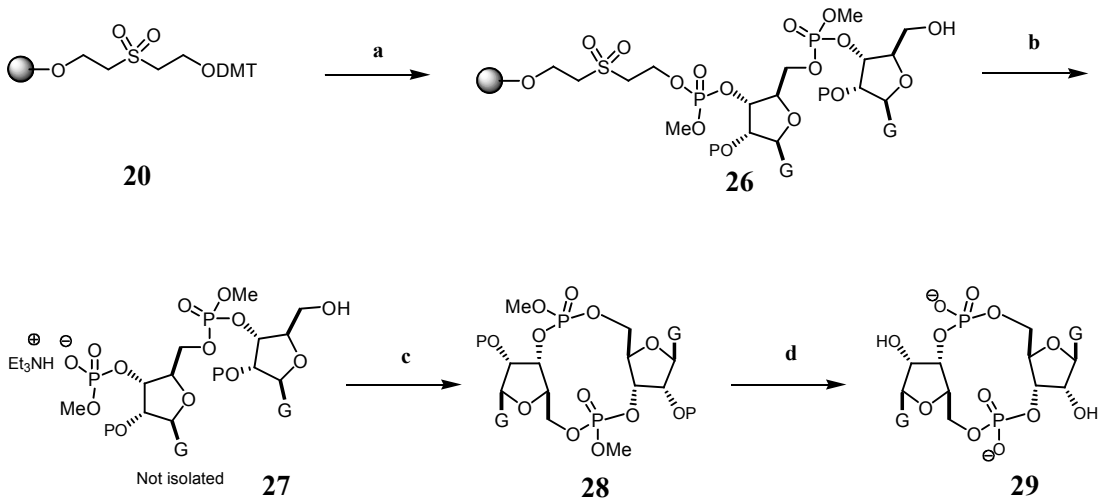

P=TBS

Scheme 6. New solid-support approach to c-di-GMP and analogs. (a) programmed synthesis on a DNA synthesizer; (b) triethylamine/CH_3CN; (c) 1-(mesitylene-2-sulfonyl)-3-nitro-1,2,4-triazole/pyridine; (d) 28% aqueous ammonium hydroxide, then triethylamine trihydrofluoride (for 2'-hydroxy analogs).

Equipped with our method, we now have access to c-di-GMP and analogs thereof to study this important signaling system. The rush to develop these chemistries illustrates the importance of c-di-GMP in bacterial signaling networks.

1.5 Unanswered Questions

Great strides have been made in the field of c-di-GMP signaling in the past decades. However, there are still important questions to be answered. Several of these questions are discussed herein.

To begin, as alluded to previously, little is known about the phosphodiesterases, which are responsible for degradation of cellular c-di-GMP.[20,25] The enzymatic mechanism by which these proteins cleave c-di-GMP is unknown. It is also worth noting that while it is has been shown that the binding of c-di-GMP to a non-catalytic site of diguanylate cyclases inhibits synthesis of c-di-GMP,[43] it has not yet been shown whether there is a mechanism by which c-di-GMP exerts a similar pattern of inhibition or even activation on phosphodiesterases.

To begin to fully understand this enzyme, its mode of action must be elucidated. A crystal structure could prove to be a starting point to glean information regarding the binding of c-di-GMP to the active site of EAL domain-containing proteins and might provide clues to the mechanism of c-di-GMP degradation. However, obtaining a crystal structure has proven challenging. Co-crystallization of PDEA with c-di-GMP in the active site is desirable; however, since c-di-GMP is cleaved upon introduction into the enzyme, a non-hydrolysable analog is needed for co-crystallization.

As mentioned previously Jones' seminal work on the polymorphism of c-di-GMP[34,35] also raises many questions: Are the different interconverting polymorphic structures of c-di-GMP biologically relevant? Do different c-di-GMP adaptor proteins bind to different polymorphic structures? Experiments that can delineate the roles of the various c-di-GMP polymorphs in the bacterial signaling network would likely unravel the role that c-di-GMP plays in modulating bacterial lifestyle changes in response to

the availability of essential metals, if in fact the various polymorphic forms exist at biologically relevant concentrations.

My work, described herein, involves the synthesis of c-di-GMP analogs as tools for beginning to answer these important questions. In 1992 it was stated that "Almost nothing is known about the mechanisms whereby c-di-GMP exerts its action on the diverse cellular functions under its control."[1] Nearly two decades later, not much has changed. The concerted efforts of chemists and biologists will help unravel the intricacies of c-di-GMP signaling. The era of the c-di-GMP signaling network has indeed begun.

Chapter 2: Design and Synthesis of c-di-GMP Analogs

2.1 Design Principles

Equipped with the tools necessary to access analogs of c-di-GMP, we set out to design a rational set of molecules which would allow exploration into some of the important questions surrounding this system. The series of analogs should allow one to discern the role of specific structural features of c-di-GMP. As a first step, we chose to explore the role of the ribose moiety in the structure of the parent c-di-GMP molecule. Does the sugar provide any important hydrogen-bonding interactions? Or is it merely a source of structural rigidity?

Ribose and deoxyribose are 5-membered rings and exist in a dynamic equilibrium of four conformations (Figure 6[44]). The two most common conformations for DNA and RNA nucleotides are the 3'-*endo* and 2'-*endo* conformations, with the 3' and 2' position out of plane and on the same side as the base, respectively. As determined by NMR spectroscopy, c-di-GMP apparently adopts a 3'*endo*, 2'*exo* puckering mode.

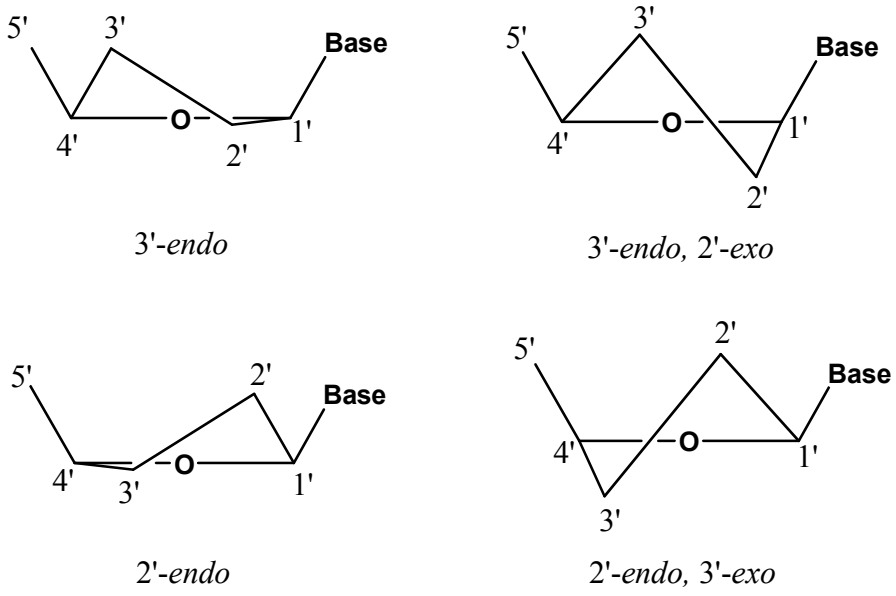

Figure 5. Common puckering modes in ribose and deoxyribose.

The analogs for this initial series are shown in Figure 6. Each molecule in this series of 2'-analogs of c-di-GMP should exhibit different hydrogen-bonding and sugar-puckering patterns. This will hopefully allow us to begin to delineate the role of the ribose in the natural compound.

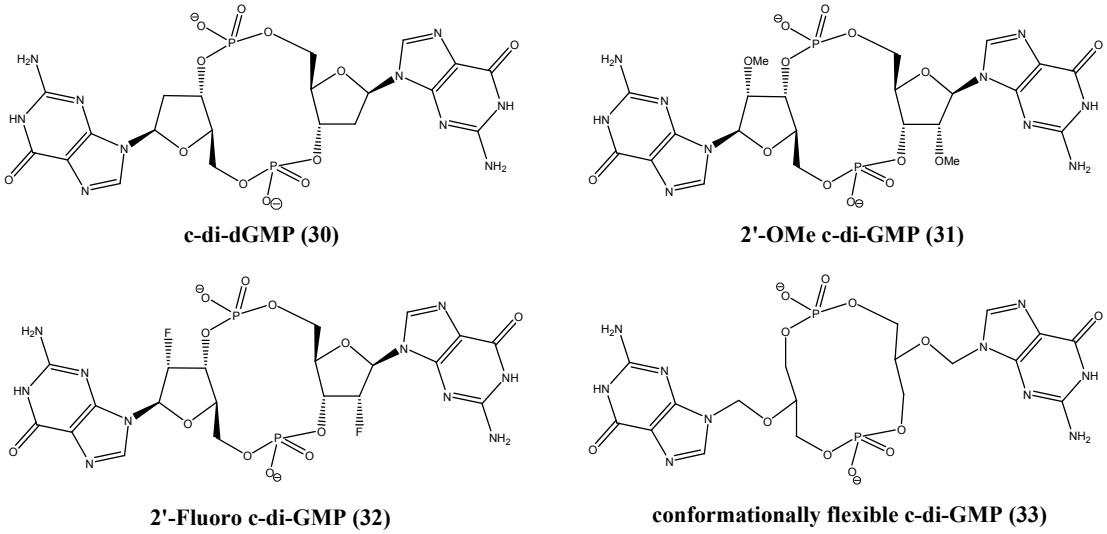

Figure 6. Family of 2' analogs of c-di-GMP.

C-di-dGMP **30**, a DNA analog of the natural c-di-GMP, should illustrate whether the 2'-OH has a role as a hydrogen-bonding partner. However, substitution of the 2'-hydroxyl group with hydrogen will result in both loss of a hydrogen-bond donor and a change in the sugar puckering as deoxyribose has all puckering modes available to it. The typical solution to this problem is to introduce a 2'-methoxy substituent. The 2'-methoxy substitution, compound **31**, is a natural progression in the family of analogs as it should exhibit the same puckering pattern as the natural analog but cannot act as a hydrogen bond donor. This molecule is also relatively easy to access from a synthetic standpoint. However, the extra sterics introduced by the methyl group should make one cautious when interpreting the results associated with the 2'-methoxy analog.

The 2'-fluoro analog **32** should provide a better isostere, as the 2'-fluorine mimics the sugar puckering character as well as the size and electronics of the hydroxyl group, yet cannot act as a hydrogen-bond donor. The 2'-fluoro substitution, however, provides a more substantial synthetic challenge. The final analog in the series, **33**, will resolve whether or not structural rigidity is a requirement for efficacy of c-di-GMP. This molecule should be completely conformationally flexible, as it is devoid of a 2'carbon in the sugar backbone portion.

In addition to these analogs, we found it convenient to also seek a complimentary set of 'hybrid' molecules, in which each bears one natural and one unnatural ribose. These analogs (Figure 7) should provide an interesting intermediary between the

structure of natural c-di-GMP and the various 2'-substituted analogs and are easily accessed by applying our synthetic methodology utilizing the natural 2'-OH phosphoramidite for the second coupling step.

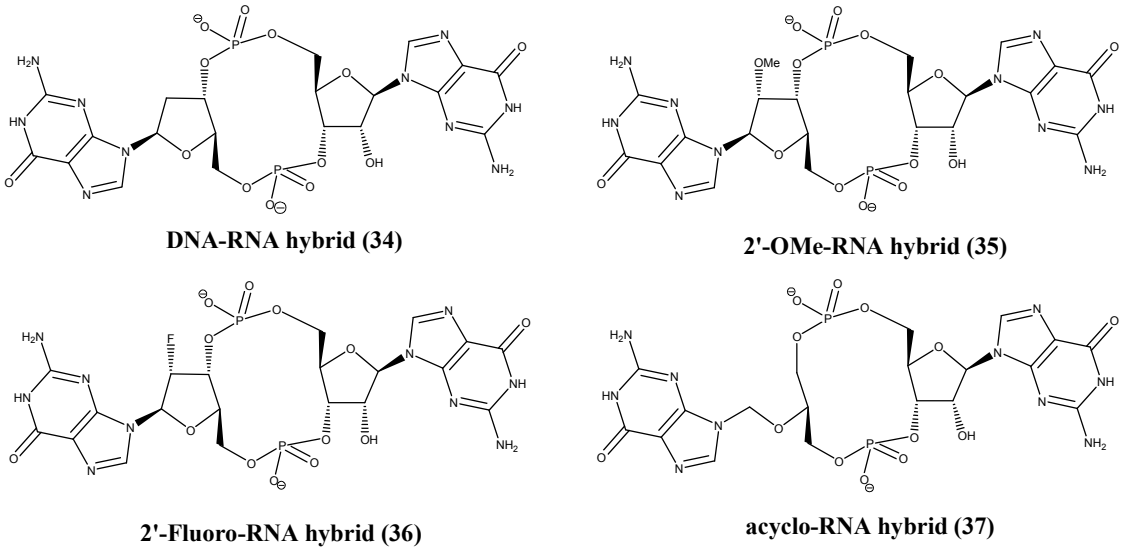

Figure 7. Family of RNA hybrid analogs of c-di-GMP.

2.2 Results and Discussion

In order to expeditiously access the family of molecules shown in Figure 7 and 8, our previously described solid-support synthesis was chosen (Scheme 6). This method should provide access to these molecules in millimolar quantities, allowing initial experiments exploring the structural role of the ribose moiety.

One shortcoming of our synthetic methodology is the use of the 3'phosphorylation CPG **20**, which can be prohibitively expensive. Currently, 20 grams of this CPG, if purchased from commercial sources costs around $5,000. Therefore, before moving

forward, we sought to synthesize this support in-house for use in our methodology. Literature revealed that the 3'-phosphate CPG can be made in two steps from 2-(4,4)-dimethoxytrityloxyethylsulfonyl)-ethanol (Scheme7).[45]

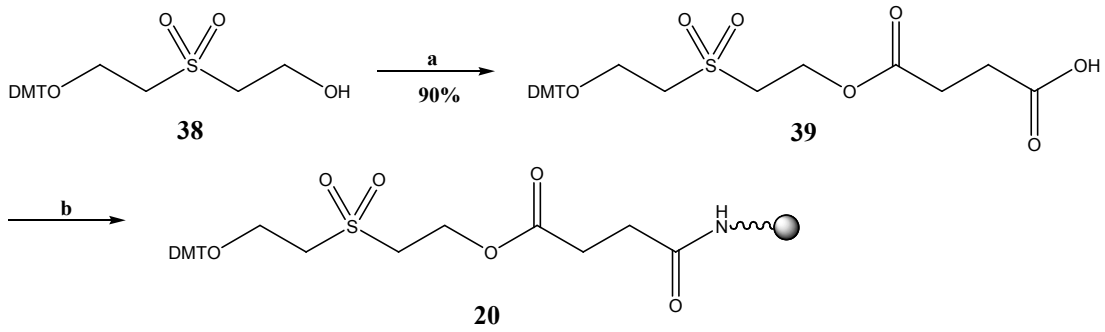

Scheme 7. Synthesis of 3'-phosphate CPG. (a) succinic anhydride, 4-dimethylaminopyridine; (b) amino CPG, 4-dimethylaminopyridine, bromotrichloromethane, triphenylphosphine.

We estimate that when synthesized via this route, 20 grams of the support costs around $300, or about 6% of the commercial cost. The synthesis was successfully carried out yielding about 100 grams of the 3'-phosphate CPG, not only to complete this work, but also for future use by the Sintim Group.

To employ our method, we must also obtain the 2'-substituted P-methoxy phosphoramidites which correspond to each compound in the series. The phosphoramidites are then dissolved in acetonitrile and carried on to the automated synthetic steps. The general structure for the P-methoxy phosphoramidite is shown in Figure 8.

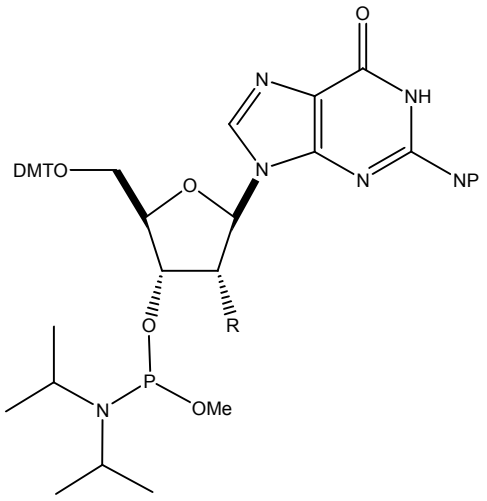

R = H, OH, OCH_3, or F

Figure 8. General structure of P-methoxy phosphoramidites.

The DNA analog, **30** (Figure 6) was synthesized first. The previously described method was employed using the synthetic 3'-phosphate CPG and the commercially available deoxyguanine P-methoxy phosphoramidite. The compound was purified by HPLC and characterized by ESI-MS (Appendix).

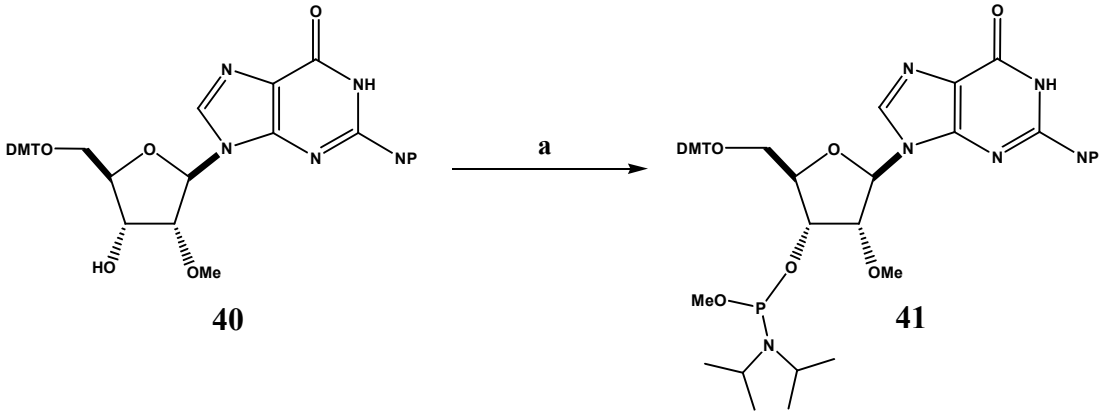

40 **41**

Scheme 8. Synthesis of 2'-OMe P-methoxy phosphoramidite. (a) N,N,N,N-tetraisopropyl-*p*-methoxy phosphoramide, tetrazole, CH_3CN.

For the synthesis of analogs **31** and **35** (Figures 6 and 7, respectively) bearing the 2'-OMe substituent, the 2'-OMe P-methoxy phosphoramidite was generated in one step from its corresponding commercially available nucleoside using a literature method (Scheme 8).[46]

The P-methoxy phosphoramidite was successfully obtained using N,N,N,N-tetraisopropyl-P-methoxy phosphoramide in the presence of tetrazole in acetonitrile. It was found that the phosphoramidites are somewhat water sensitive and can decompose without careful handling. For these reasons, the phosphoramidite was used immediately without purification or characterization. The previously described synthetic route was carried out using the synthetic phosphoramidite. The key 2'-TBS-protected intermediate was characterized by ESI-MS (Appendix) to confirm the success of the phosphorylation reaction.

The next analogs which were sought are the conformationally flexible acyclo-analogs **33** and **37** (Figures 6 and 7, respectively) which are devoid of a 2'-carbon in one or both of the ribose portions of the structure.

A search of the literature revealed a reported synthesis[47] which would be amenable to making the phosphoramidite necessary for the generation of these analogs. Although it appeared simple on paper; in practice, the synthesis (Scheme 9) would turn out to be much more challenging.

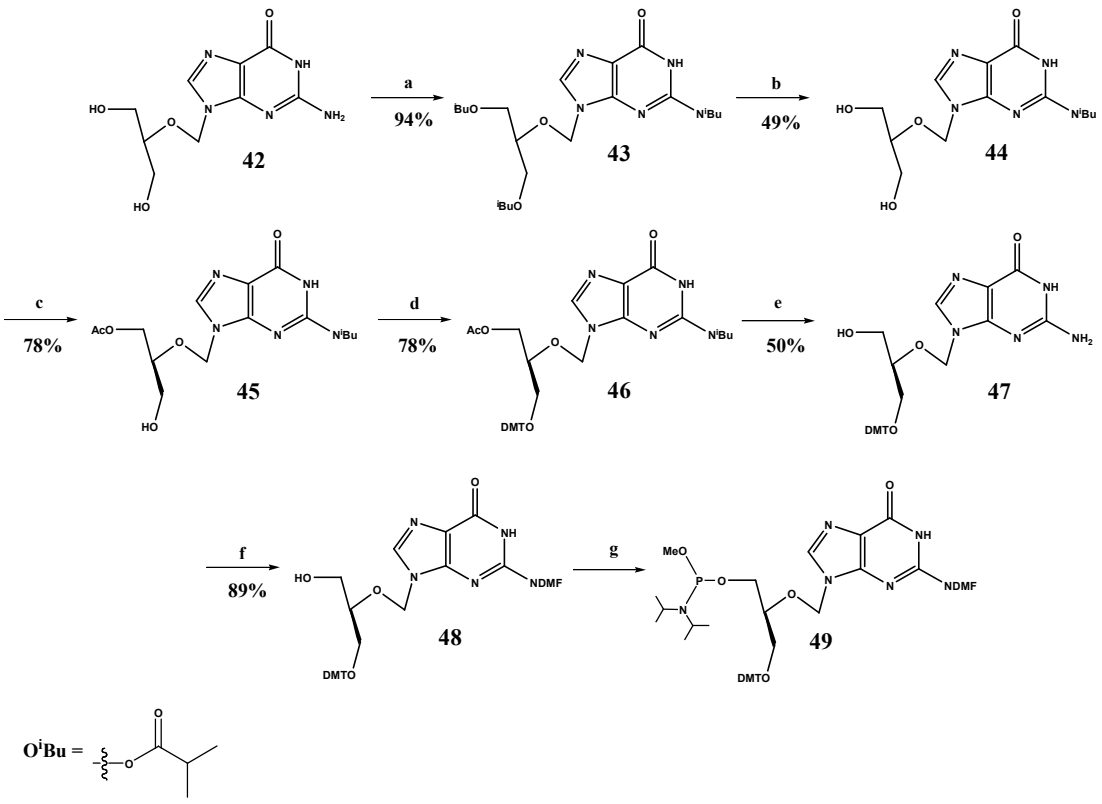

Scheme 9. Synthesis of conformationally flexible, acyclo-c-di-GMP. (a) isobutyryl chloride; (b) sodium hydroxide, hydrochloric acid; (c) lipase; (d) dimethoxytrityl chloride; (e) potassium carbonate; (f) dimethylformamide/dimethyl acetal; (g) N,N,N,N-tetraisopropyl-*p*-methoxy phosphoramide, tetrazole, CH_3CN.

Before discussing the issues that were encountered with this synthesis, it is worth noting that it is not strictly necessary to carry out an asymmetric synthesis of the acyclo phosphoramidite for synthesis of the acyclo dimer analog, due to the fact that the final analog is achiral (Figure 9). However, we initially sought this pathway to achieve the syntheses of both the dimer and its corresponding RNA hybrid analog, which requires a chiral phosphoramidite.

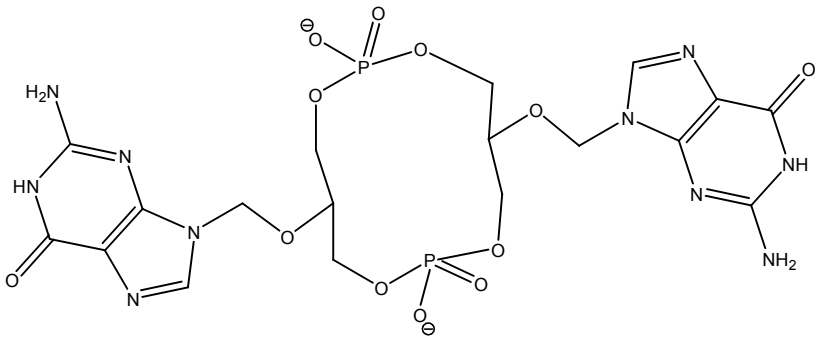

Figure 9. Conformationally flexible acyclo dimer analog of c-di-GMP.

The synthesis began with the commercially available compound 1,3-dihydroxy-2-propoxymethyl guanine (DHPG) **42**. Tri-isobutyryl protection of DHPG with isobutyryl chloride was carried out successfully with no deviation from the literature.[52] However, subsequent treatment with base to obtain the partially protected DHPG **44**, bearing two free hydroxyl functionalities, proved difficult. Often, unwanted deblocking of the exocyclic amine of the base would occur, especially in large-scale reactions. After some efforts, a re-evaluation of the literature revealed that compound **44** can be accessed directly from DHPG by a one-pot reaction utilizing chlorotrimethylsilane followed by isobutyric anhydride.[48] This reaction proved to be much more efficient.

Resolution of the meso diol **44** with porcine pancreatic lipase provided the di-protected compound **45**, in a stereoselective manner as confirmed by ^{1}H NMR. Our initial plan involved subsequent tritylation of the remaining hydroxyl moiety followed by selective deprotection under mildly basic conditions to yield the desired compound, ready for phosphorylation.

The tritylation reaction was carried out with minimal difficulty to give **46.** However, in our hands the selective deprotection again resulted in unwanted deblocking of the exocyclic amine of the base. The exocyclic amine would have to be re-protected before attempting the subsequent phosphorylation reaction. For this purpose, the N', N'-dimethylformamidine (DMF) group was chosen. The DMF group provides a facile protection of the amine in the presence of the free alcohol, thus circumventing the need for an additional protection-deprotection sequence.

The reaction was carried out successfully by treatment with dimethylformamide/dimethylacetal giving **48,** and finally the phosphorylation was carried out. As before, due to the instability of the phosphoramidite, the product was used immediately without purification or characterization.

Unfortunately, after carrying out the previously described synthetic sequence (Scheme 6), the desired compounds were not obtained. It is possible that the compounds were lost during the synthesis, but the more likely cause is that the phosphorylation reaction failed. As a result of the length of the synthesis, coupled with the number of steps requiring modification or optimization and the cost of the DHPG starting material; there was only enough material obtained to attempt one trial of the phosphorylation.

Although the penultimate compound in the synthesis was not successfully obtained; the pitfalls are now well-understood, such that a future member of the Sintim Laboratory can repeat the work using the lessons described herein as a guide.

The remaining molecules in the set are those bearing the 2'-fluoro substituent (compounds **32** and **36**, Figures 6 and 7, respectively). A review of the literature revealed that the synthesis of the 2'-fluoro-2'-deoxy guanosine moiety is non-trivial. Our search revealed a recent chemical synthesis of 2'-fluoro adenine[49] involving condensation of 1-O-acetyl-2-deoxy-2-fluoro-3,5-di-O-benzoyl-β-D-ribo-furanose[50] with N^2-palmitoyl adenine in the presence of trimethylsilyl triflate (Scheme 10).

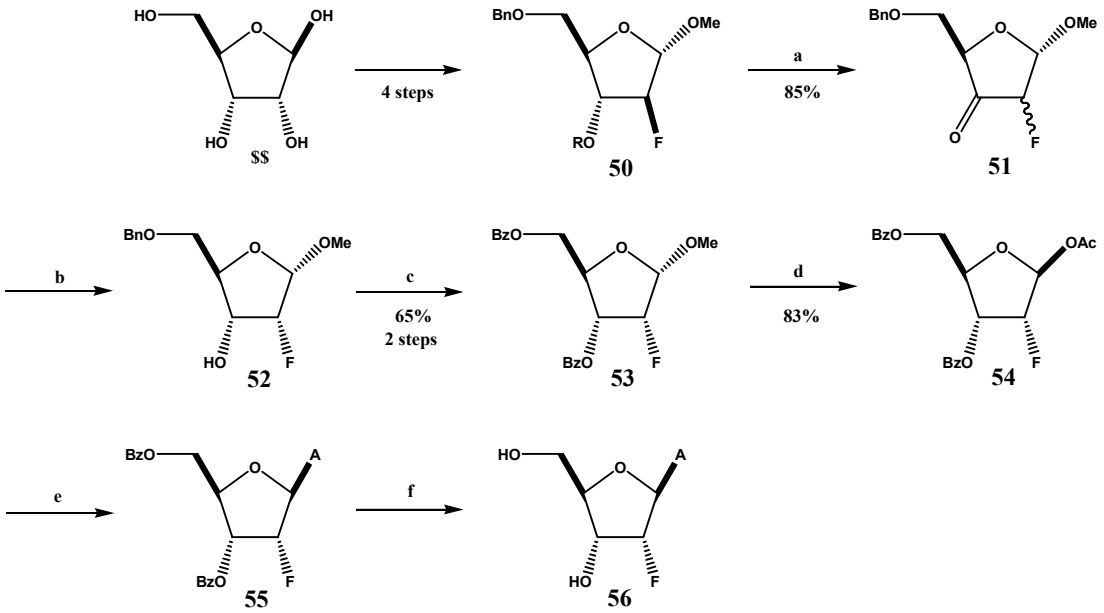

Bn = benzyl, Bz = benzoyl

Scheme 10. Reported synthesis[55] of 2'-deoxy-2'-fluoro-adenine. (a) acetic anhydride, Me_2SO; (b) sodium borohydride, CH_3CH_2OH; (c) benzoyl chloride, pyridine; (d) acetic acid, acetic anhydride, sulfuric acid; (e) 16-persilylated N_2-benzoyladenine, $SnCl_4$, CH_3CN, 1,2-dichloroethane; (f) aqueous sodium hydroxide.

Oxidation of arabinoside **50** with dimethyl sulfoxide-acetic anhydride affords a mixture of the epimeric free ketones **51**. Reduction with sodium borohydride in ethanol followed by column chromatography gives **52.** Subsequent protection of the 3'-hydroxyl group gives compound **53**, which is then converted to the acetate **54**. Treatment of the acetate with N^2-palmitoyl adenine in the presence of trimethylsilyl triflate and subsequent deprotection yields the free 2'-deoxy-2'-fluoro-adenine **56**.

There are several problems with this route that are immediately obvious. To begin, the overall yield in transforming compound **50** to our desired intermediate compound **54** is 46% over five steps. Although this seems reasonable initially, further inspection reveals that compound **50** is not commercially available. It is not discussed explicitly in the paper, but we believe that compound **50** can be accessed in a minimum of four steps from commercially available ribose. Therefore the overall length of the sequence is at best nine steps and potentially low-yielding (we do not have any information about the overall yield of steps 1-4). The length of this route, coupled with the preponderance of low-yielding and non-stereospecific steps and the number of column chromatographic separations, led us to pursue an alternative synthetic pathway.

Further search of the literature revealed that 2'-deoxy-2'-fluoro-uridine can accessed readily in two steps from the commercially available nucleotide uridine or in only one step from 2,2'-anhydro-1-(β-D-arabinofuranosyl)uracil[51], which is also commercially available. It has also been shown that uridine to guanine glycosyl transfer reactions

occur readily in the presence of N,O-bis(trimethylsilyl)acetamide and trimethylsilyltriflate in acetonitrile.[52] However, to our knowledge, no one has combined these strategies and applied them to the synthesis of 2'-deoxy-2'-fluoro-guanosine.

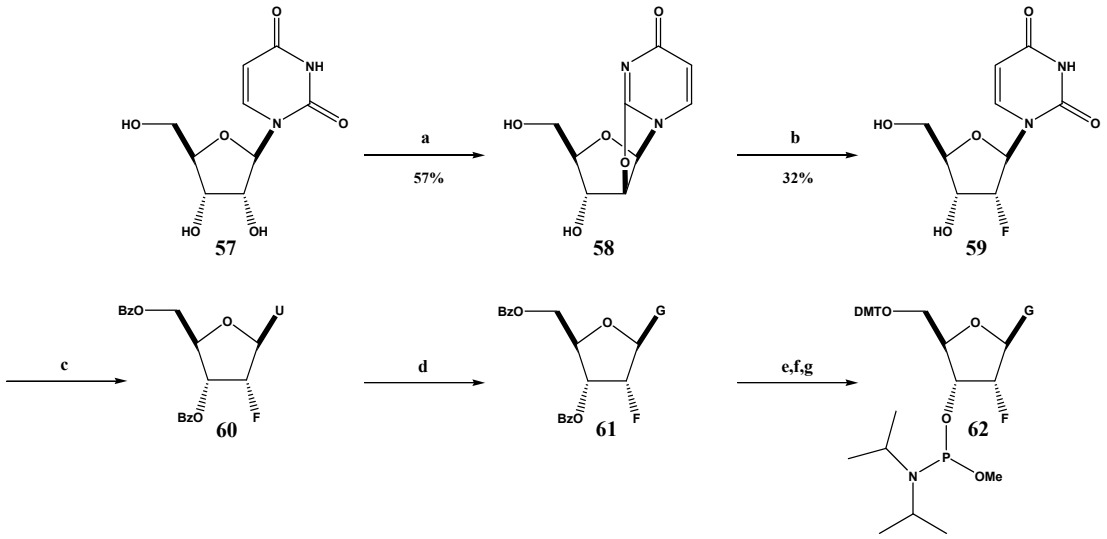

Scheme 11. Route to 2'-deoxy-2'-fluoro-guanosine and its phosphoramidite. (a) diphenyl carbonate, hexamethylphosphoramide, sodium carbonate; (b) hydrofluoric acid/pyridine; (c) benzyl chloride, pyridine; (d) N,O-Bis(TMS)acetamide, N_2isobutyryl-Guanine, trimethylsilyl triflate; (e) H_2/Pd; (f) dimethoxytrityl chloride; (g) *N,N,N,N*-tetraisopropyl-P-methoxy phosphoramide, tetrazole, CH_3CN.

Therefore, we sought a novel synthetic route to 2'-fluoro-substituted guanosine, employing a U to G transglycosylation reaction as the key step, which is a significant improvement over current methods (Scheme 11). This sequence should provide the key intermediate **60**, ready for the transglycosylation in two steps from the commercially available compound **58.**

Due to cost considerations, we opted to synthesize compound **58** in-house. Treatment of uridine **57** with diphenyl carbonate in HMPA, in the presence of sodium carbonate

provided 2,2'-anhydro-1-(β-D-arabinofuranosyl)uracil **58** in 57% yield. Stereoselective ring opening to **59** was achieved in 32% yield by heating in HF/pyridine in sealed plastic centrifuge tubes.

Our plan for the remaining synthesis involves benzyl-protection of the free hydroxyl groups followed by transglycosylation, leading to the desired 2'-deoxy-2'-fluoro-guanosine. The synthesis will be completed by tritylation of the product followed by phosphorylation providing the p-methoxy phosphoramidite for the solid-support synthesis of the corresponding c-di-GMP analog.

2.3 Conclusions

The Sintim laboratory has developed a solid-support methodology which is amenable to synthesis of a wide scope of c-di-GMP analogs. The issue of the cost-effectiveness of the method has now been solved by synthesizing the 3'-phosphate CPG in-house. A phosphorylation reaction, which should be amenable to future work in the Sintim Laboratory, was also successfully applied to the synthesis of the 2'-OMe P-methoxy phosphoramidite.

Although the synthesis of the acyclo phosphoramidite was unsuccessful, the intricacies of the reactions involved have been elucidated for application by a future member of the group. A robust synthesis of the final intermediate prior to phosphorylation has been achieved. Further, the groundwork has also been laid for the synthesis of the 2'-fluoro phosphoramidite, the synthetic approach to which is

described herein. Additionally, a significant amount of the key intermediate, 2'-fluoro-2'-deoxyuridine, was accessed for this purpose.

2.4 Future Work in the Sintim Group

Future work in the Sintim Group will involve the application of synthetic routes described herein to the completion the analog series. Further work will involve the use of these analogs to study of the mechanism of degradation by PDE-A.

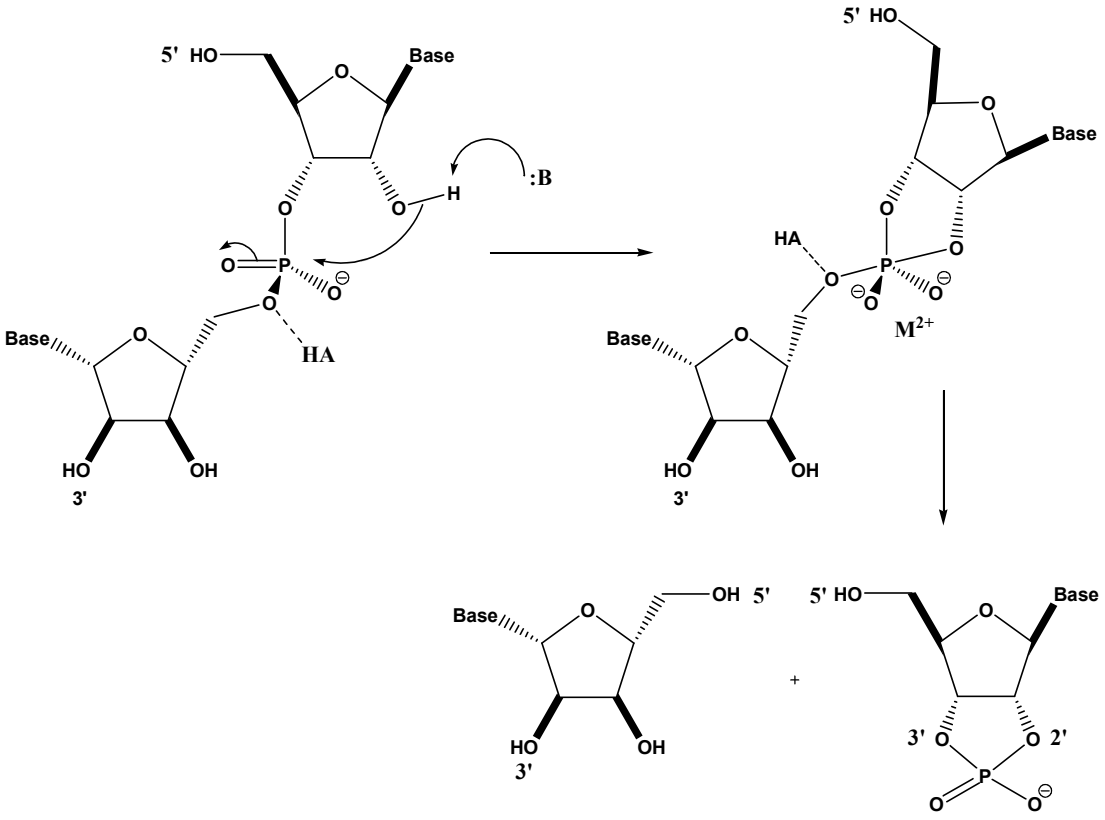

Figure 10. General mechanism for RNA hydrolysis.

The general mechanism for an RNAse degradation of ribonucleotides is shown in Figure 10.[53] In this mechanism, attack of oxygen on phosphorus forms a trigonal

bipyramidal transition state. The transition state falls apart to form the cleaved products. For RNA hydrolysis, the nucleophile can be the 2'-OH of the ribose moiety, resulting in a cyclic 2',3'-phosphate moiety.

In an alternative mechanism (Figure 11), attack of oxygen on phosphorus performs a direct S_N2 displacement of the 5'-phosphorylated fragment leading to the formation of the same cleavage products. In this case, there is no observed trigonal bipyramidal transition state.

A third possibility is that an external hydroxyl group from deprotonated water or a nucleophilic side chain in the nuclease enzyme can act as the nucleophile in the attack on the phosphorus, yielding a 5'-phosphate and a 3'-hydroxyl. This mechanism (Figure 12[39]) can act on both DNA and RNA. Note that this mechanism may also occur via an S_N2-type pathway (not shown).

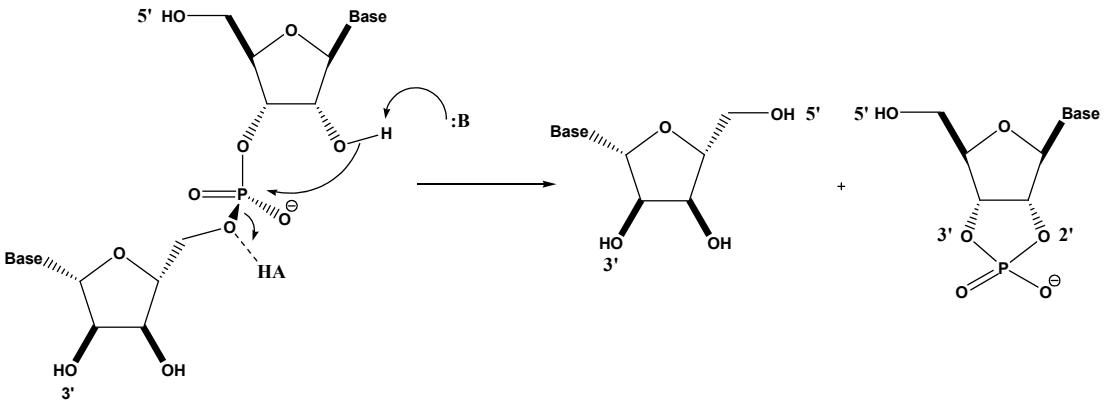

Figure 11. S_N2 mechanism for RNA degradation by intramolecular pathway.

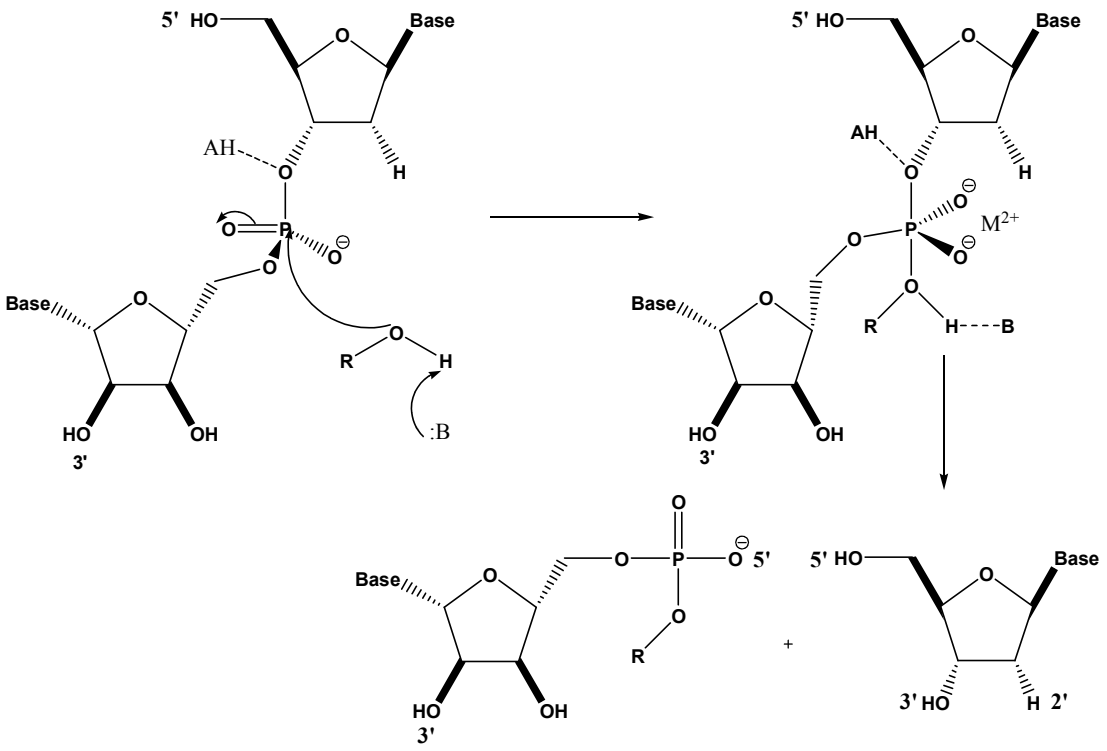

Figure 12. Mechanism for hydrolysis by an external nucleophile.

One might assume that because c-di-GMP is an RNA oligomer, the mode of hydrolysis is of the RNAse-type. However, this mechanism is dependent on the ability of the 2'-OH to approach the phosphorus in the first intramolecular step. After examination of the sugar puckering patterns of the ribose moiety in DNA and RNA nucleotides, and further analysis of the structure of c-di-GMP, one might instead predict a DNAse-type cleavage. The key question is how might we begin to delineate among these various possibilities?

We hope that this work has provided the tools necessary to access these analogs which will ultimately allow us to discern among these possibilities. We can begin to establish whether cleavage of c-di-GMP takes place by an RNAse-type mechanism or

by a DNAse-type mechanism involving an external hydroxyl nucleophile and also whether a direct S_N2 displacement is occurring. Further, we hope to discover whether the 2' hydroxyl moiety is necessary for structural rigidity or rather as an internal nucleophile. Detailed binding and kinetic experiments on the PDEA enzymes will be required to answer these questions.

These analogs may also allow us to observe the role of the various polymorphs described by Jones'. If for example we find that a particular analog is biologically active, but unable to form higher order aggregates, we can conclude that such aggregates are biologically irrelevant. Conversely, if such analogs are less active, we might infer that the aggregation is necessary for activity or that possible the aggregate itself is the active form.

Chapter 3: Experimental

3.1 General Materials and Methods

All reactions were carried out under a nitrogen or argon atmosphere, using anhydrous solvents and oven-dried glassware, unless otherwise noted. Syringes were oven-dried and cooled *in vacuo*. Commercially available compounds were used as obtained, unless otherwise noted. Compounds were purchased from one of the following: Sigma-Aldrich, VWR, Toronto Research Chemicals, Fisher Scientific, or Acros Organics. Anhydrous solvents were obtained as follows: dichloromethane, pyridine, and acetonitrile were distilled from calcium hydride under an argon atmosphere; benzene, dimethylformamide, and triethylamine, were dried over activated molecular sieves. Reactions were stirred magnetically and monitored by multi-lane analysis thin-layer chromatography on Sorbent Technologies 200 micron aluminum-backed plates. Thin-layer chromatography plates were visualized using UV (254 nm) or stains where appropriate. Automated syntheses were carried out on an Applied Biosystems 392 DNA/RNA Synthesizer. All yields refer to chromatographically and spectroscopically pure compounds, unless otherwise noted. Compounds were purified via either silica gel chromatography, using standard grade, 230x400 mesh Sorbent Tech silica gel and specified solvents as mobile phase or by high pressure liquid chromatography using a Varian ProStar HPLC and mixtures of water or ammonium carbonate buffer and acetonitrile.

Compounds were characterized by one or more of the following methods: ^{1}H, ^{13}C, and ^{19}F NMR, and mass spectrometry. Compounds with a literature precedent were compared to previously obtained spectroscopic data. Nuclear magnetic resonance spectra were obtained using a 400 MHz Bruker Avance Nuclear Magnetic Resonance (NMR) Spectrometer utilizing d-chloroform, d-methanol, or deuterium oxide as solvent, as noted, and are referenced by the relevant solvent residual peak. Mass spectral data was obtained using either a Finnigan TSQ Quantum Discovery Max Mass Spectrometer or an Applied Biosystems QSTAR/Pulsar Mass Spectrometer.

3.2 General Procedures

Solid-support synthesis of cyclic oligonucleotides Commercial or synthetic phosphoramidites are dissolved in anhydrous acetonitrile to obtain a final concentration of approximately 1 M. Automated synthesis of the linear dinucleotide coupled to the 3'-phosphate CPG is then carried out using the DNA synthesizer. Subsequent cleavage of the linear dimer from the solid-support is achieved by treatment of the resin with ~30% triethylamine in anhydrous acetonitrile for 5 h. The resin is then recovered by filtration and re-subjected to cleavage overnight. The combined filtrates are concentrated *in vacuo,* dried by co-evaporation with anhydrous pyridine and suspended in anhydrous pyridine to which 1-(mesitylene-2-sulfonyl)-3-nitro-1,2,4-triazole is added (final concentration ~0.1 M). The reaction is stirred at room temperature for ~48 h. After 48 h, the reaction mixture is concentrated *in vacuo* and the residue is re-suspended in 28-30% aqueous ammonium hydroxide. After heating at 55 ^{o}C on a heating block for 18 h, the ammonia is removed by heating at 65

^{o}C for ~2 h open to the atmosphere. The sample is then filtered and purified by HPLC. Compounds containing the 2'-TBS moiety are subsequently treated with 200 µL triethylamine trihydrofluoride in 200 µL DMSO and heated at 65 ^{o}C for 2.5 h after which the reaction is quenched by addition of 1.3 mL of TRIS RNA quenching buffer, filtered, and purified by HPLC using a reverse phase C_{18} column by gradient elution (0-90% acetonitrile:ammonium carbonate) at 25 ˚C.

3.3 Chemical Procedures

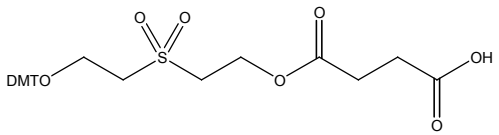

39

Mono 2-dimethoxytrityloxyethanesulfonyl)-ethyl succinate[45] (39) To a stirred solution of 2-(dimethoxytrityloxyethylsulfonyl)-ethanol (1.00 g, 2.19 mmol) and dimethylaminopyridine (281 mg, 2.30 mmol) in dichloromethane (9 mL), was added succinic anhydride (230 mg, 2.30 mmol). The reaction was stirred at ambient temperature for 30 min. After this time, the reaction mixture was diluted with dichloromethane, washed with 0.5 M potassium phosphate (pH = 5) and water, dried over sodium sulfate, filtered, and concentrated *in vacuo* yielding **39** (1.10 g, 1.98 mmol, 90%) as a white crystalline solid. This material was used without any further purification or characterization. **P085AS (Notebook reference).**

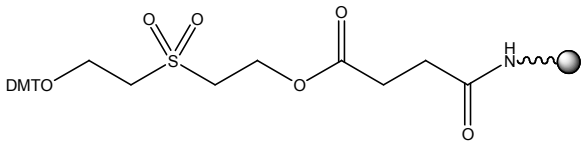

20

3'-Phosphorylation CPG[45] (20) Mono 2-(4,4)-dimethoxytrityloxyethanesulfonyl)-ethyl succinate **39** (4.48 g, 8.05 mmol) was suspended in acetonitrile (160 mL), to which were added sequentially bromotrichloromethane (3.98 g, 20.1 mmol) and dimethylaminopyridine (1.95 g, 15.9 mmol). To this mixture was added a solution of triphenylphosphine (1.05 g, 4.00 mmol) in acetonitrile (80 mL). The mixture was stirred for 30 s after which the amino CPG was added. The heterogeneous mixture was stirred at ambient temperature for 30 min. At this time, the functionalized resin was recovered on a sintered glass funnel, washed with acetonitrile and diethyl ether, and dried *in vacuo.* Unfunctionalized amino groups were capped by treatment with commercial capping solution (equal parts Cap A and Cap B containing acetic anhydride/triethylamine/N-methylimidazole/dichloromethane) for 30 min at ambient temperature to cap unreacted amino groups. The functionalized resin was again recovered on a sintered glass funnel, washed with acetonitrile and diethyl ether, and dried *in vacuo.* The reaction product was confirmed by a small-scale detritylation with trichloroacetic acid in dichloromethane resulting in the formation of an intense orange color.

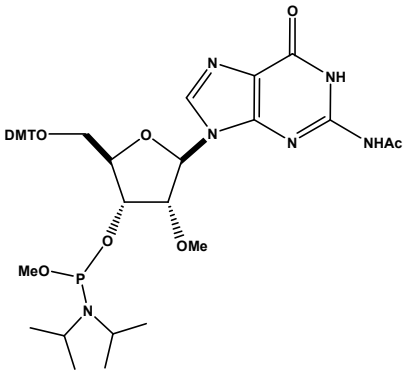

41

N-Ac-rG-2'OMe P-methoxy phosphoramidite[46] (41) To an oven-dried 50-mL round-bottom flask was added N-Ac-rG-2'OMe nucleoside (1.00 g, 1.56 mmol). The material was co-evaporated with anhydrous pyridine, dried *in vacuo* for 2 h, and suspended in anhydrous acetonitrile (6 mL). To this was added N,N,N,N-tetraisopropyl-p-methoxy phosphoramide (450 mg, 1.72 mmol). The reaction mixture was cooled to 0 ˚C and tetrazole (3.80 mL, 0.45 M in acetonitrile) was added. The reaction mixture was stirred for 5 min after which, it was allowed to warm to ambient temperature and stirred for 1 h. At this time, the reaction was filtered into an oven-dried glass vessel and carried on to the automated syntheses without any further purification or characterization. **P097AS.**

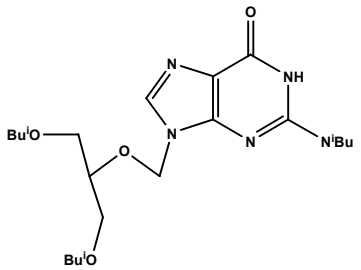

43

Triisobutyryl-DHPG[47] (43) A 50-mL round-bottom flask was charged with 1,3-dihydroxy-2-propoxymethyl guanine (DHPG) (1.00 g, 3.92 mmol) and pyridine (16

mL) and cooled to 0 °C in an ice-water bath. Isobutyryl chloride (1.66 g, 15.7 mmol) was added to the mixture dropwise via syringe over 5 min. The reaction mixture was allowed to warm to ambient temperature and stirred for 18 h. After complete conversion of starting material as judged by TLC, the mixture was poured over ice. The mixture was then concentrated *in vacuo,* and the resultant product was purified via column chromatography using 100% ethyl acetate. Fractions containing the product were combined and concentrated. Removal of solvent *in vacuo* yielded **43** (1.71 g, 3.69 mmol, 94%) as a slightly yellow solid. **^{1}H NMR** (400 MHz, $CDCl_3$, δ): 7.72 (s, 1H), 5.50 (s, 2H), 4.23 (m, 2H), 4.15 (m, 3H), 2.64 (h, 1H, *J*=8.0), 2.51 (h, 2H, *J*=11.2), 1.28 (d, 6H, *J*=6.8), 1.13 (dd, 12H, *J*=4.8). **^{13}C NMR** (100 MHz, $CDCl_3$, δ): 177.45, 155.77, 148.80, 139.27, 121.57, 77.14, 72.66, 63.21, 36.90, 34.30, 19.32. **P002AS**.

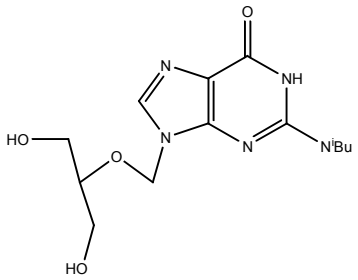

44

N-isobutyryl-DHPG[47] (44) To a 10-mL round-bottom flask containing methanol (0.5 mL) and pyridine (2.15 mL) at 0 °C, was added triisobutyryl-DHPG **43** (200 mg, 0.431 mmol). 2 M sodium hydroxide was added to the reaction mixture to obtain a pH of 13.5. After conversion of starting material as indicated by TLC, the pH was adjusted to 8 by dropwise addition of 2 M hydrochloric acid. DOWEX (strongly acidic cation exchange) resin was suspended in 20% aqueous pyridine. After 20 min,

the suspension was poured through a fritted funnel, creating a DOWEX pad through which the reaction mixture was poured and collected. The pad was washed with methanol and the flow through and washings were combined. The mixture was then concentrated *in vacuo,* and the resultant product was purified via column chromatography using gradient elution (10-30%) methanol in chloroform. Fractions containing the product were combined and concentrated. Removal of solvent *in vacuo* yielded **44** (131 mg, 0.431 mmol, 94%) as a yellow solid.

N-isobutyryl-DHPG[47] (44) To a solution of 1,3-Dihydroxy-2-propoxymethyl guanine (DHPG) (1.00 g, 3.92 mmol) in anhydrous pyridine (20 mL) was added chlorotrimethylsilane (3.8 mL) dropwise at 0 ˚C over 5 min. The mixture was allowed to warm to ambient temperature and monitored by TLC. Upon complete disappearance of starting material as indicated by TLC, the mixture was once again cooled to 0 ˚C, isobutyric anhydride (3.25 mL) was added, and stirring was resumed at ambient temperature for 18 h. At this time, the mixture was returned to 0 ˚C and cold water (18 mL) was added followed by 28% aqueous ammonium hydroxide (7.5 mL) and the mixture was stirred at ambient temperature for 1 h. Upon complete conversion as indicated by TLC, the mixture was concentrated *in vacuo.* The resultant residue was dissolved in water. The aqueous layers were washed with ethyl acetate (3 x 15 mL), filtered, and concentrated *in vacuo.* The resultant product was purified via column chromatography using gradient elution (10-20%) methanol in chloroform. Fractions containing the product were combined and concentrated. Removal of solvent *in vacuo* yielded **44** (625 mg, 1.93 mmol, 49%) as a slightly

yellow solid. **^{1}H NMR** (400 MHz, CD_3OD, δ): 8.11 (s, 1H), 5.50 (s, 2H), 3.75 (m, 1H), 3.46 (m, 1H), 2.71 (m, 1H), 1.22 (d, 6H, *J*=6.8). **^{13}C NMR** (100 MHz, MeOD, δ): 181.45, 147.14, 142.21, 81.28, 61.70, 36.01, 18.34. **P009AS**.

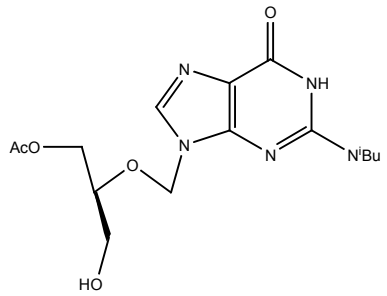

45

(S)-O-acetyl-N-isobutyryl-DHPG[47] (45) To a 250-mL round-bottom flask containing pyridine (45 mL) and benzene (22 mL) was added N-isobutyryl-DHPG **44** (300 mg, 0.898 mmol). Vinyl acetate (9 mL) and porcine pancreatic lipase (9 g) were added and the reaction was stirred at ambient temperature for 18 h. Upon disappearance of starting material, the reaction mixture was filtered and concentrated *in vacuo.* The resultant product was purified via column chromatography using gradient elution (0-20%) methanol in chloroform. Fractions containing the product were combined and concentrated. Removal of solvent *in vacuo* yielded **45** (256 mg, 0.697 mmol, 78%) as a light brown oil. **^{1}H NMR** (400 MHz, CD_3OD, δ): 8.06 (s, 1H), 5.62 (s, 2H), 4.10 (d, 1H, *J*=8.4), 3.94 (m, 2H), 3.57 (m, 2H), 3.36 (m, 1H), 2.70 (q, 1H, *J*=6.8), 1.85 (s, 3H), 1.21 (d, 6H, *J*=6.8). **P022AS**.

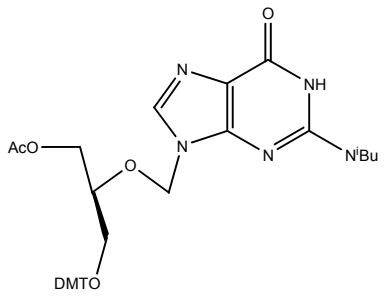

46

(S)-DMT-O-acetyl-N-isobutyryl-DHPG[47] (46) A 10-mL round-bottom was charged with (S)-O-acetyl-N-isobutyryl-DHPG **45** (256 mg, 0.687 mmol) and dichloromethane (3.5 mL). To this stirring mixture were added sequentially Hunig's base (diisopropylethylamine) (0.73 mL), dimethoxytrityl chloride (472 mg, 1.39 mmol), and dimethylaminopyridine (8.5 mg, 0.07 mmol). The reaction was stirred at ambient temperature and monitored by TLC. After complete conversion of the starting material, the reaction was quenched by addition to water and diluted with dichloromethane (5 mL). The aqueous layers were extracted with dichloromethane (3 x 15 mL). The combined organic layers were washed with water (3 x 15 mL), dried over sodium sulfate, filtered, and concentrated *in vacuo.* The resultant product was purified via column chromatography (silica neutralized with 1% triethylamine) using gradient elution (0-2%) methanol in dichloromethane. Fractions containing the product were combined and concentrated. Removal of solvent *in vacuo* yielded **46** (362 mg, 0.541 mmol, 78%) as a slightly orange solid. **^{1}H NMR** (400 MHz, CD_3OD, δ): 7.75 (s, 1H), 7.30 (m, 9H), 6.82 (d, 4H, *J*=8.8), 5.57 (s, 2H), 4.12 (d, 2H, *J*=5.6), 3.89 (q, 1H, *J*=8.0), 3.20 (m, 2H), 2.80 (s, 6H), 1.93 (s, 3H), 1.18 (d, 6H, *J*=6.8). **P025AS**.

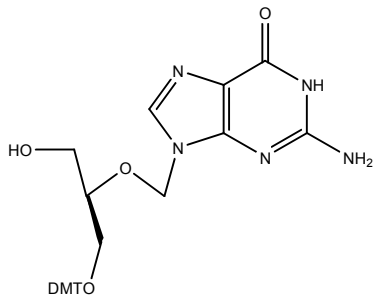

47

(S)-DMT-DHPG (47) (S)-DMT-O-acetyl-N-isobutyryl-DHPG **46** (60 mg, 0.09 mmol) was suspended in 5% potassium carbonate (1.1 mL), which was previously prepared by addition of 5 g of potassium carbonate to 60 mL methanol and 40 mL water. The reaction was stirred at ambient temperature and monitored by TLC. After 30 min the reaction was diluted with dichloromethane, washed with water (3 x 15 mL), dried over sodium sulfate, filtered, and concentrated *in vacuo.* The resultant product was purified via column chromatography (silica neutralized with 1% triethylamine) using gradient elution (0-5%) methanol in dichloromethane. Fractions containing the product were combined and concentrated. Removal of solvent *in vacuo* yielded **47** (28 mg, 0.045 mmol, 50%) as a slightly yellow solid. **^{1}H NMR** (400 MHz, CD_3OD, δ): 7.86 (s, 1H), 7.25 (m, 9H), 6.78 (d, 4H, *J*=8.4), 5.58 (s, 2H), 3.96 (s, 2H), 3.55 (q, 1H, *J*=8.0), 3.40 (m, 2H), 3.00 (s, 6H). **P024AS.**

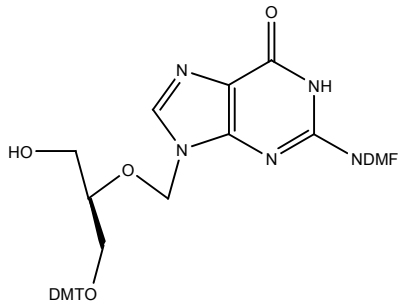

48

(S)-DMT-N-DMF-DHPG[54] (48) To a stirring solution of (S)-DMT-DHPG **47** (50 mg, 0.09 mmol) in dry dimethylformamide (2 mL) was added dimethylformamide dimethylacetal (0.2 mL). The mixture was stirred at ambient temperature and monitored by TLC. After 3 h, the reaction mixture was concentrated *in vacuo* and purified via column chromatography (silica neutralized with 1% triethylamine) using 8% methanol in dichloromethane. Fractions containing the product were combined and concentrated. Removal of solvent *in vacuo* yielded **48** (49 mg, 0.08 mmol, 89%) as an off-white solid. **^{1}H NMR** (400 MHz, CD_3OD, δ): 8.39 (s, 1H), 7.66 (s, 1H), 7.29 (m, 9H), 6.77 (d, 4H, *J*=8.4), 5.58 (s, 2H), 3.96 (s, 2H), 3.00 (s, 6H), 3.55 (q, 1H, *J*=8.0), 3.40 (m, 2H), 2.94 (s, 3H), 2.63 (s, 3H). **P117AS.**

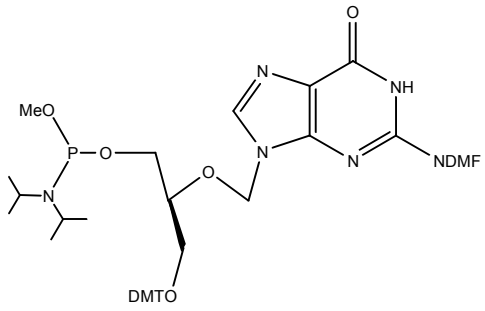

49

(S)-DMT-N-DMF-DHPG-O-P-methoxy phosphoramidite (49) To an oven-dried 50-mL round-bottom flask was added (S)-DMT-N-DMF-DHPG **48** (96 mg, 0.157

mmol). The material was co-evaporated with anhydrous pyridine, dried *in vacuo* for 2 h, and suspended in anhydrous acetonitrile. To this was added N,N,N,N-tetraisopropyl-P-methoxy phosphoramide (45 mg, 0.172 mmol). The reaction mixture was cooled to 0 ˚C and tetrazole (0.37 mL, 0.45 M in acetonitrile) was added. The reaction mixture was stirred for 5 min after which, it was allowed to warm to ambient temperature and stirred for 1 h. At this time, the reaction was filtered into an oven-dried vessel and carried on to the automated syntheses without any further purification or characterization. **P121AS.**

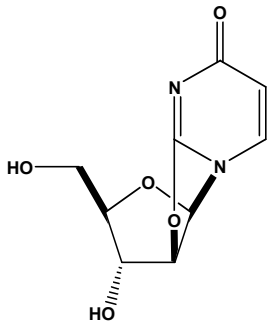

58

2,2'-anhydro-1-(*β*-D-arabinofuranosyl)uracil[51] (58) To a solution of uridine (10 g, 41.0 mmol) and diphenyl carbonate (11.4 g, 53.24 mmol) in hexamethylphosphoramide (HMPA) was added sodium bicarbonate (344 mg, 4.1 mmol). The reaction was stirred at 150 ˚C and monitored by TLC. After 20 min, the mixture was cooled, added to water, and extracted with chloroform. The aqueous layer was concentrated *in vacuo,* and the resultant product was recrystallized from methanol yielding **58** (5.3 g, 23.43 mmol, 57%) as a slightly off-white powdery solid. **^{1}H NMR** (400 MHz, D_2O, δ): 7.32 (d, 1H, *J*=7.6), 6.41 (d, 1H, *J*=5.6), 5.26 (d, 1H,

J=5.6), 4.50-3.50 (m, 6H). **^{13}C NMR** (100 MHz, D_2O, δ): 176.02, 161.91, 138.88, 109.95, 91.55, 90.12, 90.05, 75.55, 61.14. **P124AS.**

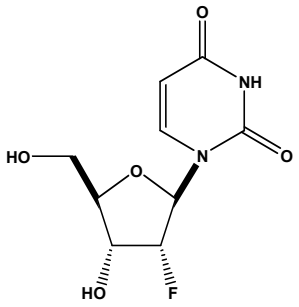

59

2'-fluoro-2'-deoxyuridine[52] (59) To a solution of 2,2'-anhydro-1-(*β*-D-arabinofuranosyl)uracil **58** (25 mg, 0.11 mmol) in anhydrous 1,4-dioxane (1.2 mL) was added hydrofluoric acid:pyridine complex (0.4 mL). The mixture was stirred in a sealed plastic screw-capped vial at 100 ˚C for 48 h. The reaction was then cooled to ambient temperature, and quenched by careful addition of excess solid calcium carbonate. The mixture was stirred for 24 h, after which the solid was filtered and washed with methanol. The combined filtrates were concentrated *in vacuo,* and the resultant product was purified via column chromatography using 20% methanol in dichloromethane. Fractions containing the product were combined and concentrated. Removal of solvent *in vacuo* yielded **59** (8.6 mg, 0.04 mmol, 32%) as a slightly yellow solid. **^{1}H NMR** (400 MHz, CD_3OD, δ): 7.83 (d, 1H, *J*=8.4), 6.11 (d, 1H, *J*=4.4), 5.63 (d, 1H, *J*=8.0), 4.20-3.50 (m, 5H). **^{13}C NMR** (100 MHz, D_2O, δ): 165.48, 151.19, 143.25, 99.93, 86.55, 85.45, 76.63, 76.00, 61.52. **^{19}F NMR** (100 MHz, D_2O, δ): -80.23. **P136AS.**

Appendix

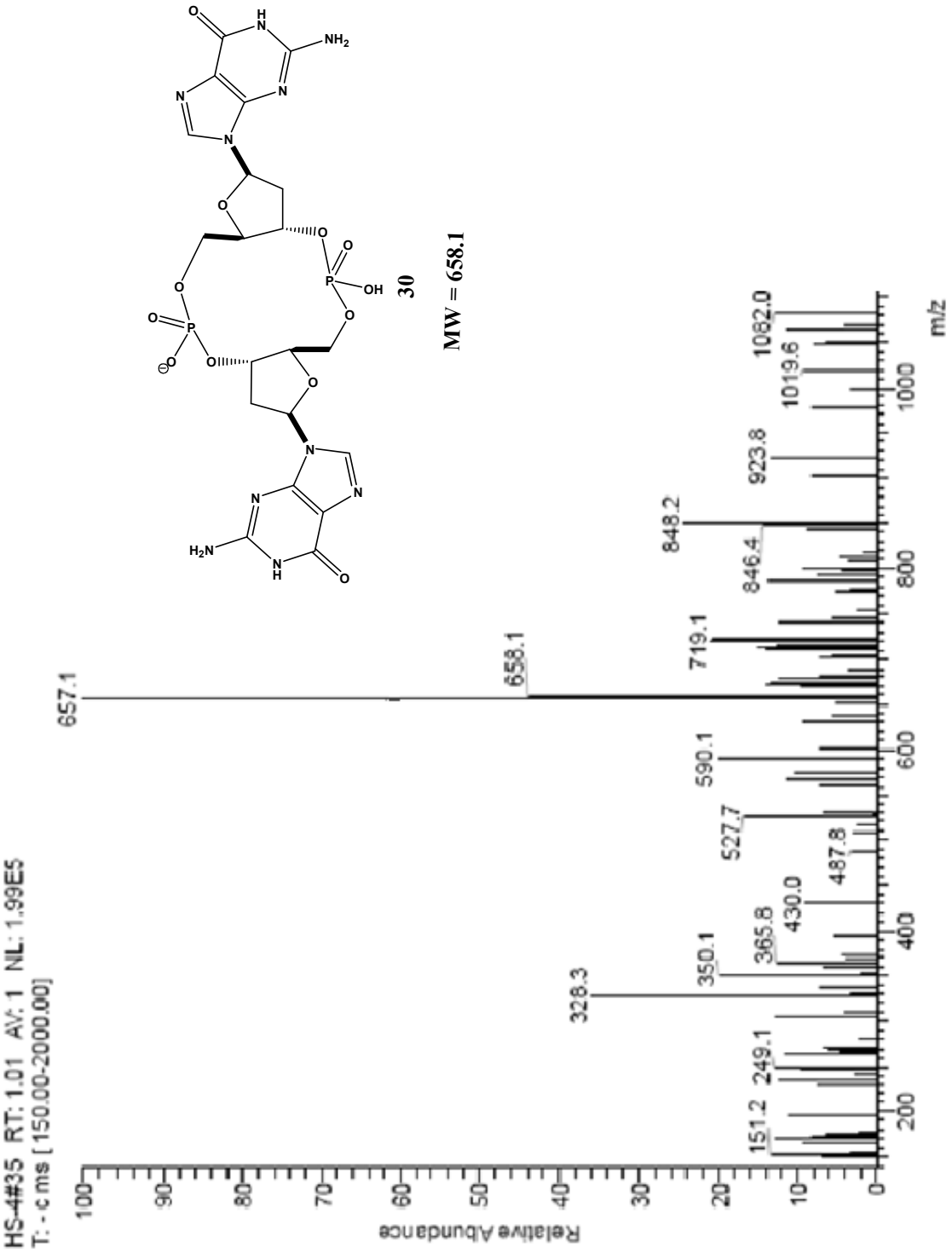
HS-4#35 RT: 1.01 AV: 1 NL: 1.99E5
T: - c ms [150.00-2000.00]
Relative Abundance
m/z
657.1
658.1
719.1
848.2
846.4
923.8
1019.6
1082.0
590.1
527.7
487.8
430.0
365.8
350.1
328.3
249.1
151.2

30

MW = 658.1

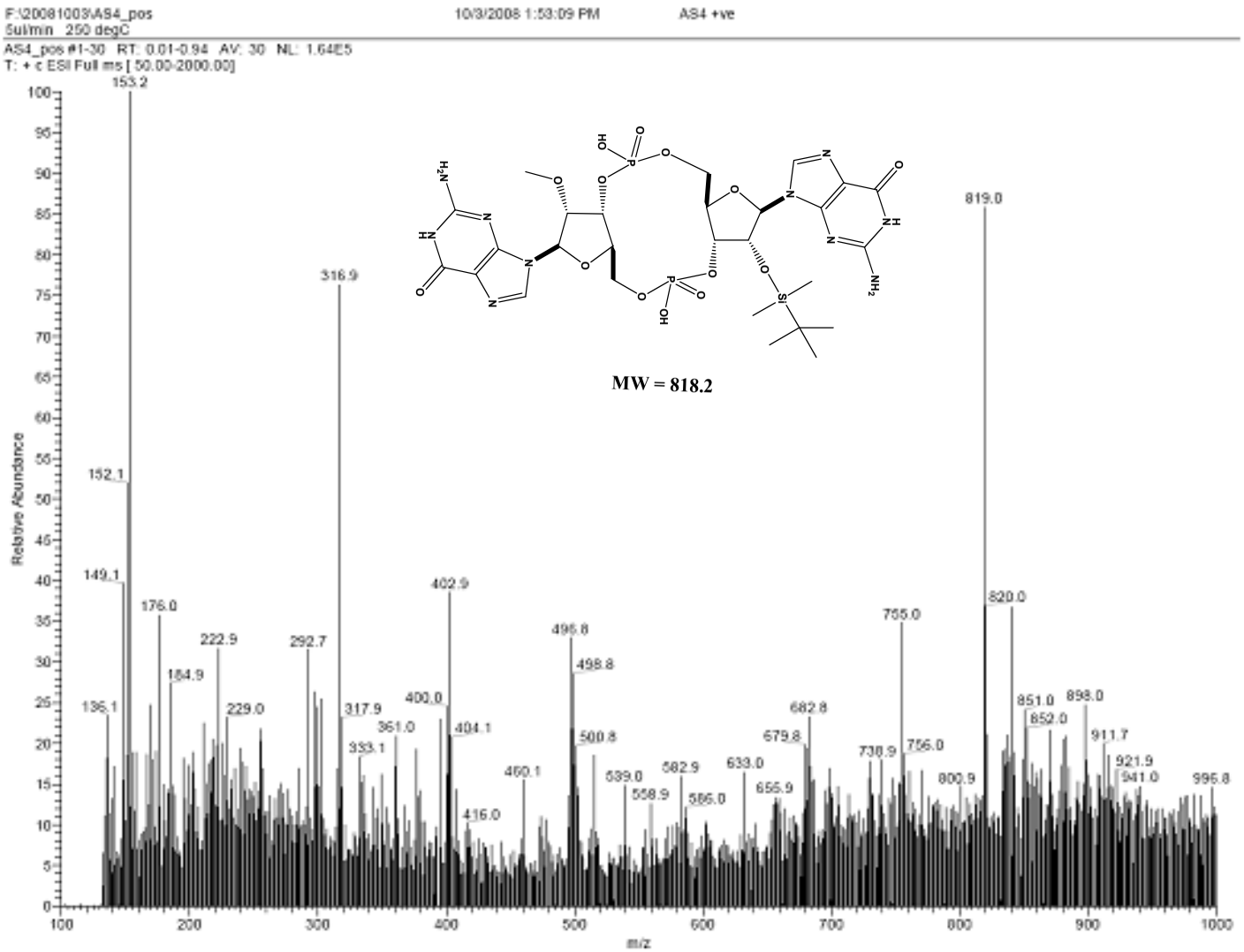
F:\20081003\AS4_pos
Sulmin 250 degC
10/3/2008 1:53:09 PM
AS4 +ve
AS4_pos #1-30 RT: 0.01-0.94 AV: 30 NL: 1.64E5
T: + c ESI Full ms [50.00-2000.00]
MW = 818.2
Relative Abundance
m/z

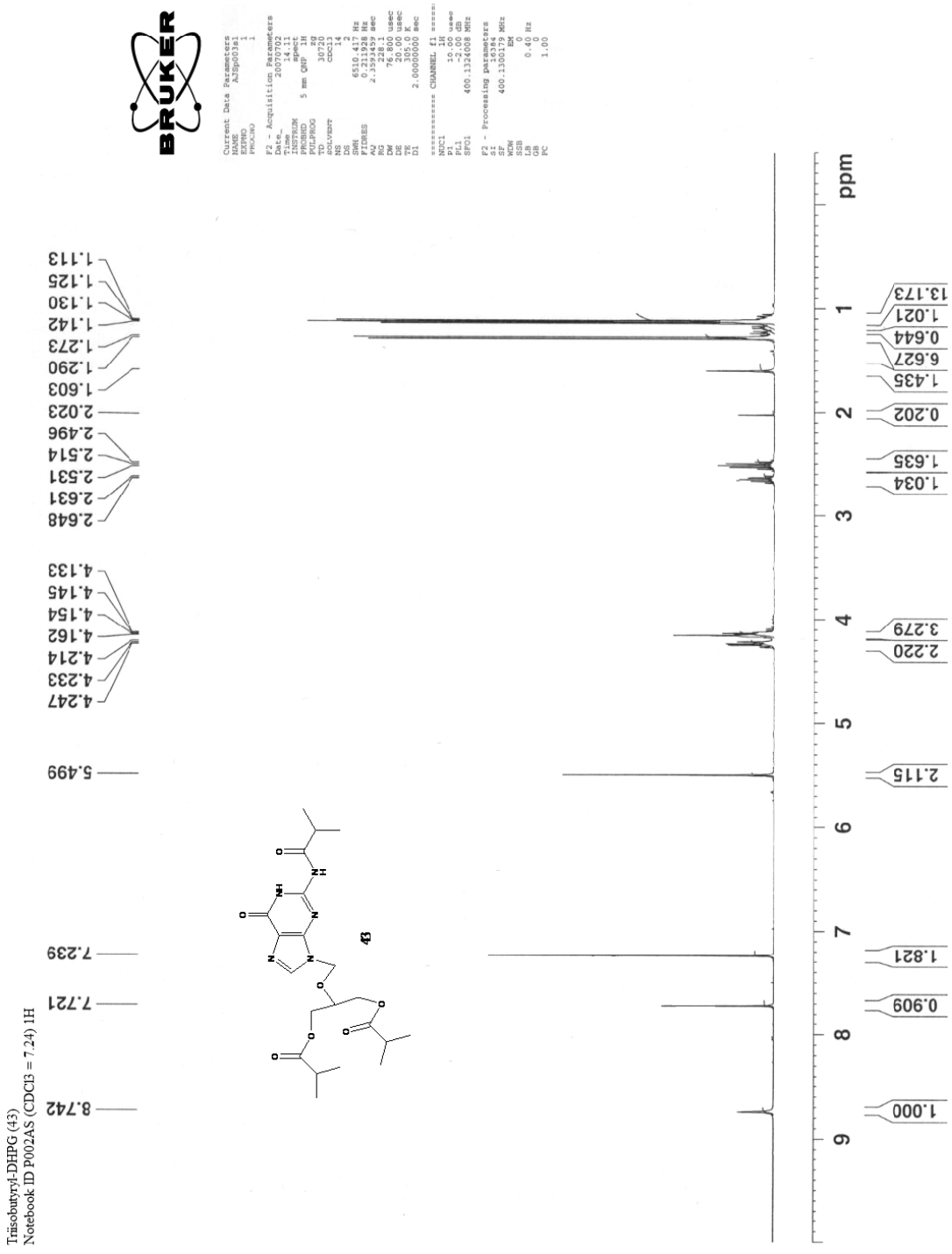
Trisobutyryl-DHPG (43)
Notebook ID P002AS (CDCl3 = 7.24) 1H
43
ppm

Triisobutyryl-DHPG (43)
Notebook ID P002AS (CDCl3) 13C

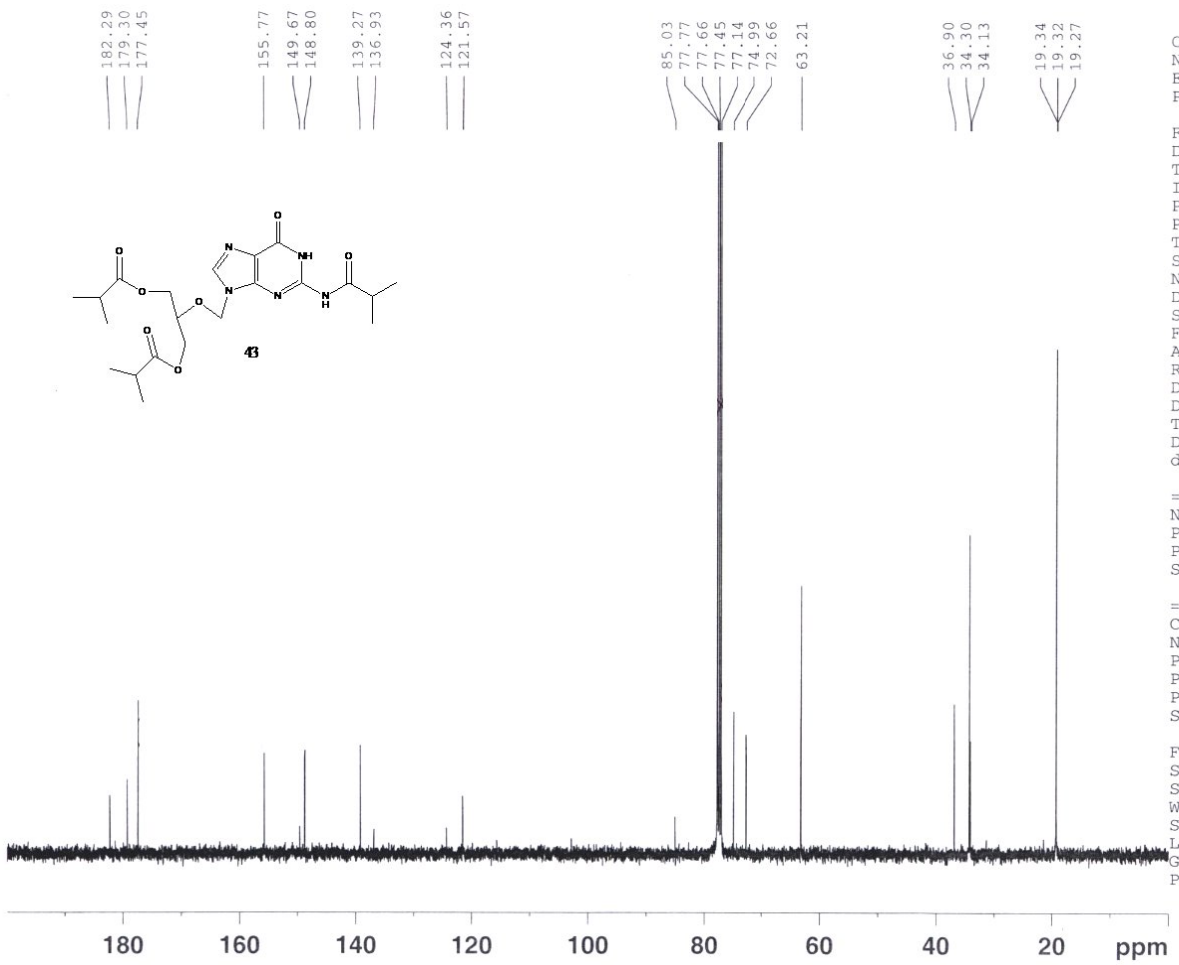

BRUKER

```
Current Data Parameters
NAME        7-wjxin-0628
EXPNO                 11
PROCNO                 1

F2 - Acquisition Parameters
Date_           20070628
Time               12.45
INSTRUM            spect
PROBHD   5 mm QNP  1H/1
PULPROG          zgdc30
TD                65536
SOLVENT           CDCl3
NS                 1300
DS                    4
SWH           27173.912 Hz
FIDRES         0.414641 Hz
AQ             1.2059124 sec
RG                287.4
DW               18.400 usec
DE                6.00 usec
TE                300.0 K
D1            1.50000000 sec
d11           0.03000000 sec

======== CHANNEL f1 ========
NUC1                13C
P1                 4.60 usec
PL1                0.00 dB
SFO1        100.5242095 MHz

======== CHANNEL f2 ========
CPDPRG2         waltz16
NUC2                1H
PCPD2          116.00 usec
PL2             -4.00 dB
PL12            17.64 dB
SFO2        399.7315989 MHz

F2 - Processing parameters
SI                32768
SF          100.5121480 MHz
WDW                EM
SSB                   0
LB                 1.00 Hz
GB                    0
PC                 1.40
```

Triisobutyryl-DHPG (43)
Notebook ID P002AS (CDCl3) DEPT135

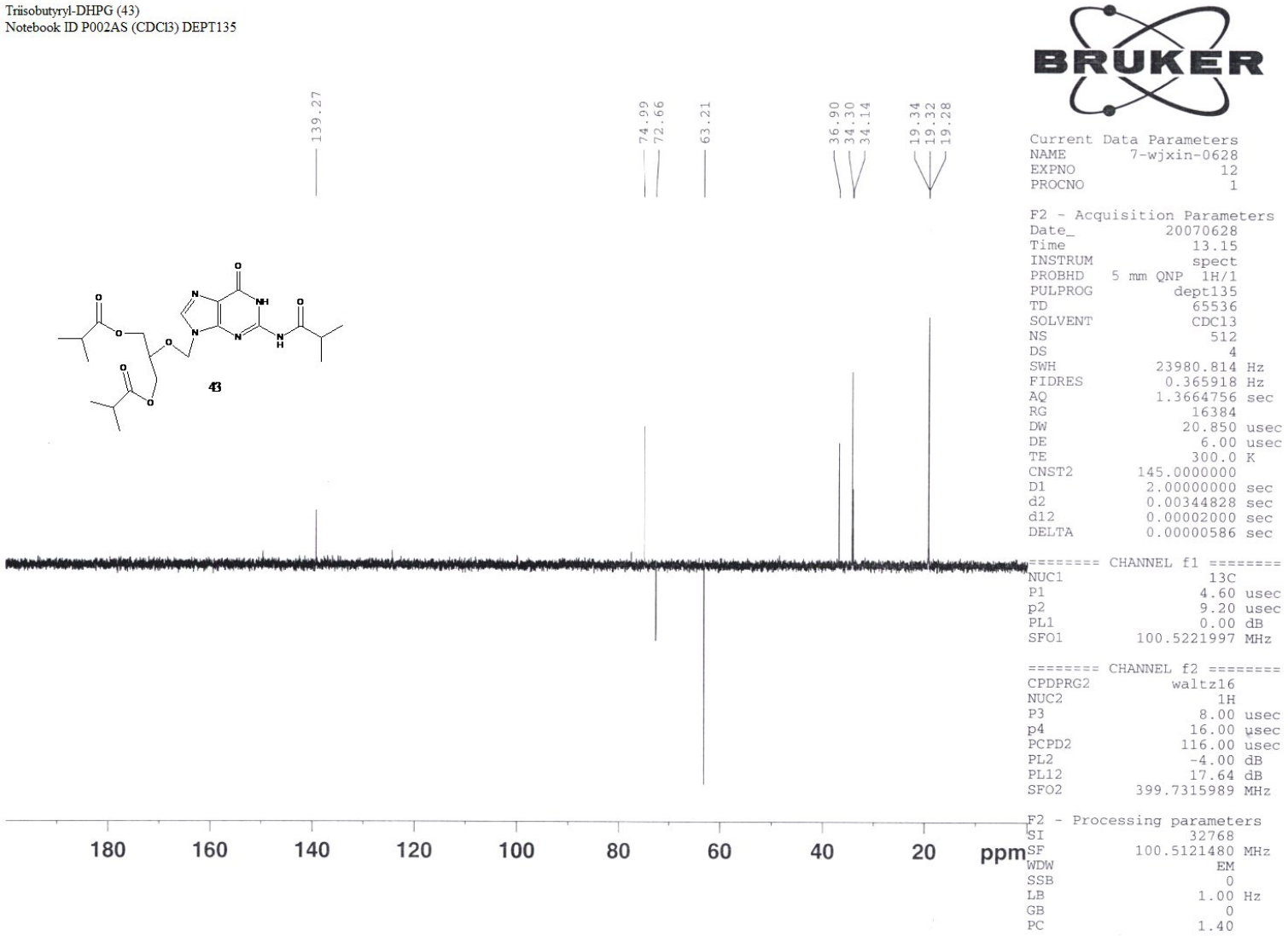

BRUKER

Current Data Parameters
NAME 7-wjxin-0628
EXPNO 12
PROCNO 1

F2 - Acquisition Parameters
Date_ 20070628
Time 13.15
INSTRUM spect
PROBHD 5 mm QNP 1H/1
PULPROG dept135
TD 65536
SOLVENT CDC13
NS 512
DS 4
SWH 23980.814 Hz
FIDRES 0.365918 Hz
AQ 1.3664756 sec
RG 16384
DW 20.850 usec
DE 6.00 usec
TE 300.0 K
CNST2 145.0000000
D1 2.00000000 sec
d2 0.00344828 sec
d12 0.00002000 sec
DELTA 0.00000586 sec

======== CHANNEL f1 ========
NUC1 13C
P1 4.60 usec
p2 9.20 usec
PL1 0.00 dB
SFO1 100.5221997 MHz

======== CHANNEL f2 ========
CPDPRG2 waltz16
NUC2 1H
P3 8.00 usec
p4 16.00 usec
PCPD2 116.00 usec
PL2 -4.00 dB
PL12 17.64 dB
SFO2 399.7315989 MHz

F2 - Processing parameters
SI 32768
SF 100.5121480 MHz
WDW EM
SSB 0
LB 1.00 Hz
GB 0
PC 1.40

N-isobutyryl-DHPG (44)
Notebook ID P009AS (MeOD = 4.87) 1H

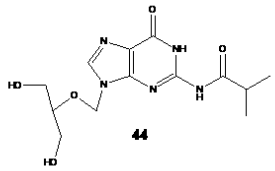

BRUKER

```
Current Data Parameters
NAME                  as1009
EXPNO                      1
PROCNO                     1

F2 - Acquisition Parameters
Date_              20070712
Time                  14.32
INSTRUM               spect
PROBHD     5 mm QNP  1H
PULPROG                 zg
TD                     30720
SOLVENT                MeOH
NS                        16
DS                         2
SWH                6510.417 Hz
FIDRES             0.211928 Hz
AQ                 2.3593459 sec
RG                      20.5
DW                   76.800 usec
DE                   20.00 usec
TE                   305.0 K
D1                2.00000000 sec

============ CHANNEL f1 ============
NUC1                      1H
P1                   10.00 usec
PL1                  -2.00 dB
SFO1           400.1324008 MHz

F2 - Processing parameters
SI                     16384
SF             400.1300179 MHz
WDW                       EM
SSB                        0
LB                   0.40 Hz
GB                         0
PC                    1.00
```

(S)-O-acetyl-N-isobutyryl-DHPG (45)
Notebook ID P022AS (MeOD = 4.87) 1H

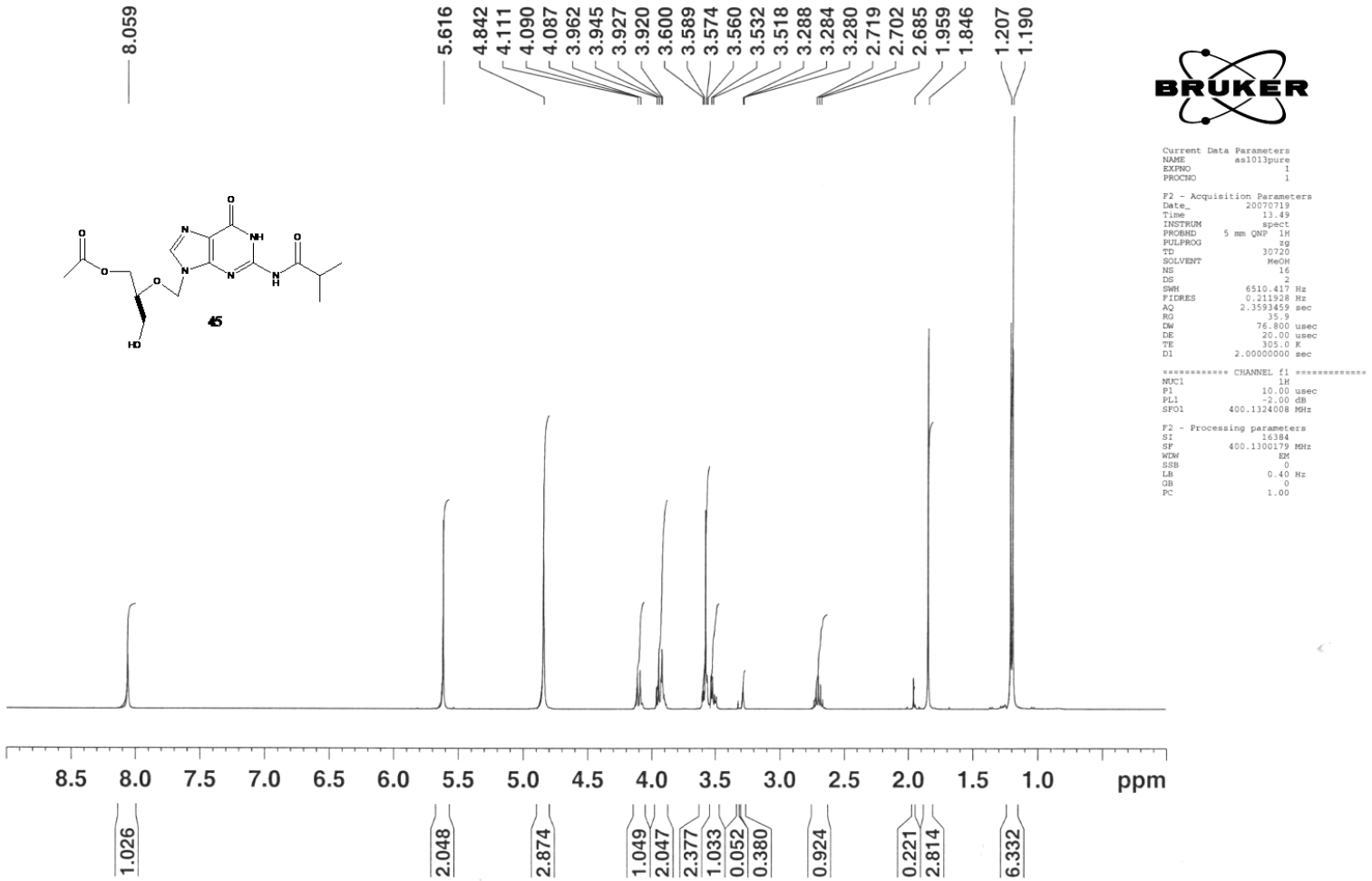

(S)-DMT-O-acetyl-N-isobutyryl-DHPG (46)
Notebook ID P025AS (CDCl3 = 7.24) 1H

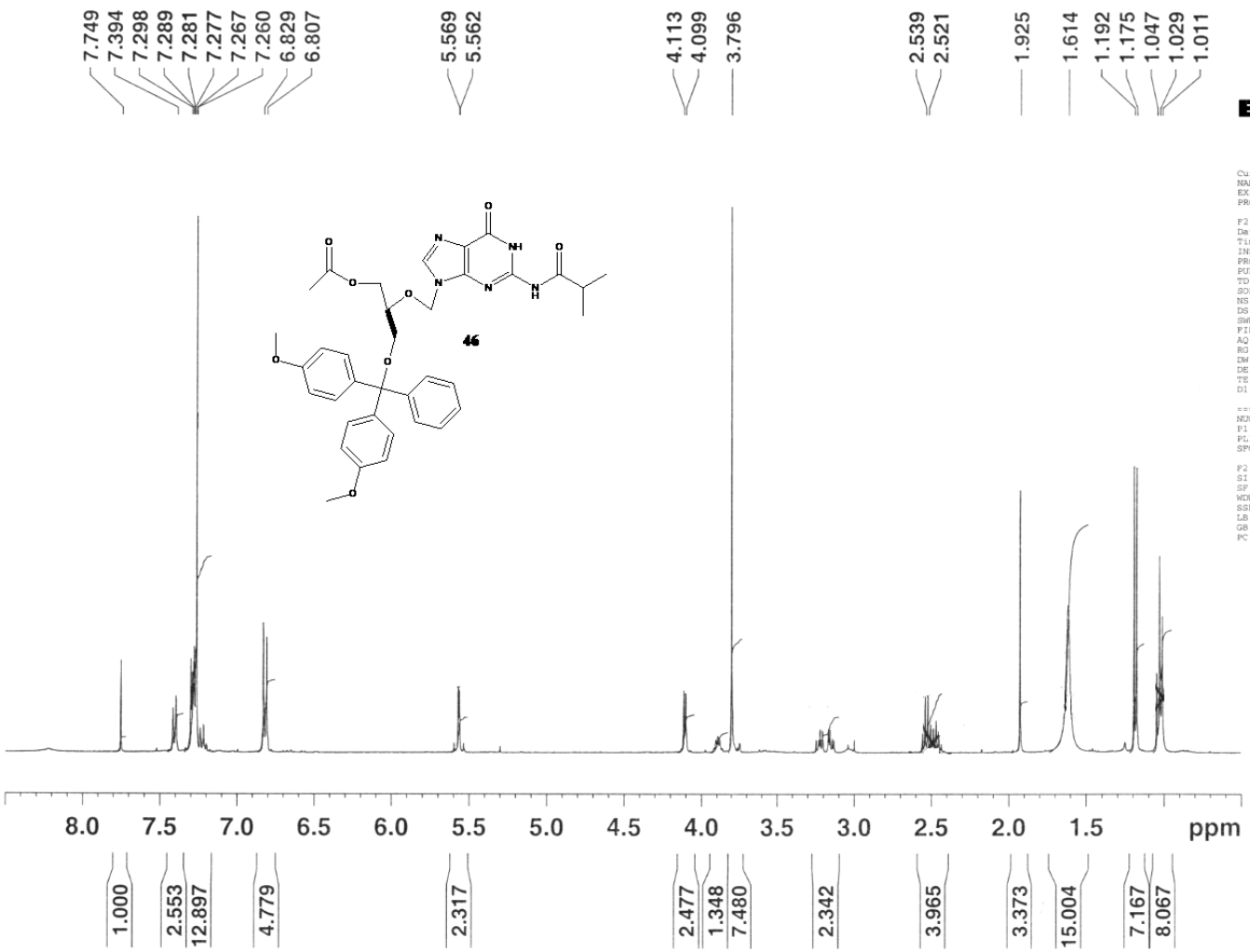

BRUKER

```
Current Data Parameters
NAME          as1023pure
EXPNO                  1
PROCNO                 1

F2 - Acquisition Parameters
Date_           20070802
Time               12.45
INSTRUM            spect
PROBHD     5 mm QNP  1H
PULPROG               zg
TD                 30720
SOLVENT            CDCl3
NS                    16
DS                     2
SWH             6510.417 Hz
FIDRES          0.211928 Hz
AQ              2.3593459 sec
RG                   256
DW                76.800 usec
DE                20.00 usec
TE                305.0 K
D1             2.00000000 sec

============ CHANNEL f1 =============
NUC1                  1H
P1                 10.00 usec
PL1                -2.00 dB
SFO1          400.1324008 MHz

F2 - Processing parameters
SI                 16384
SF            400.1300092 MHz
WDW                   EM
SSB                    0
LB                  0.40 Hz
GB                     0
PC                  1.00
```

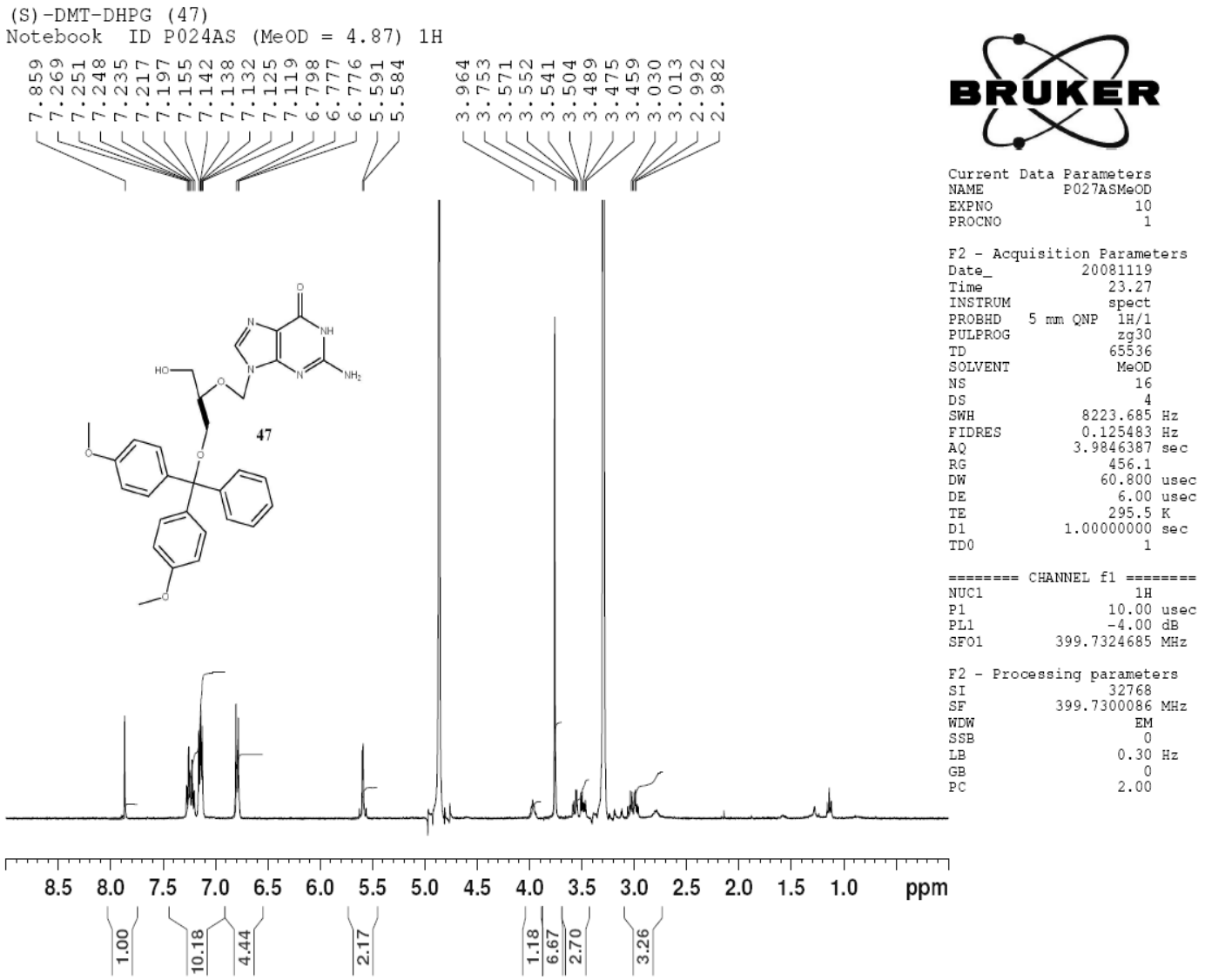

BRUKER

Current Data Parameters
NAME P027ASMeOD
EXPNO 10
PROCNO 1

F2 - Acquisition Parameters
Date_ 20081119
Time 23.27
INSTRUM spect
PROBHD 5 mm QNP 1H/1
PULPROG zg30
TD 65536
SOLVENT MeOD
NS 16
DS 4
SWH 8223.685 Hz
FIDRES 0.125483 Hz
AQ 3.9846387 sec
RG 456.1
DW 60.800 usec
DE 6.00 usec
TE 295.5 K
D1 1.00000000 sec
TD0 1

======== CHANNEL f1 ========
NUC1 1H
P1 10.00 usec
PL1 -4.00 dB
SFO1 399.7324685 MHz

F2 - Processing parameters
SI 32768
SF 399.7300086 MHz
WDW EM
SSB 0
LB 0.30 Hz
GB 0
PC 2.00

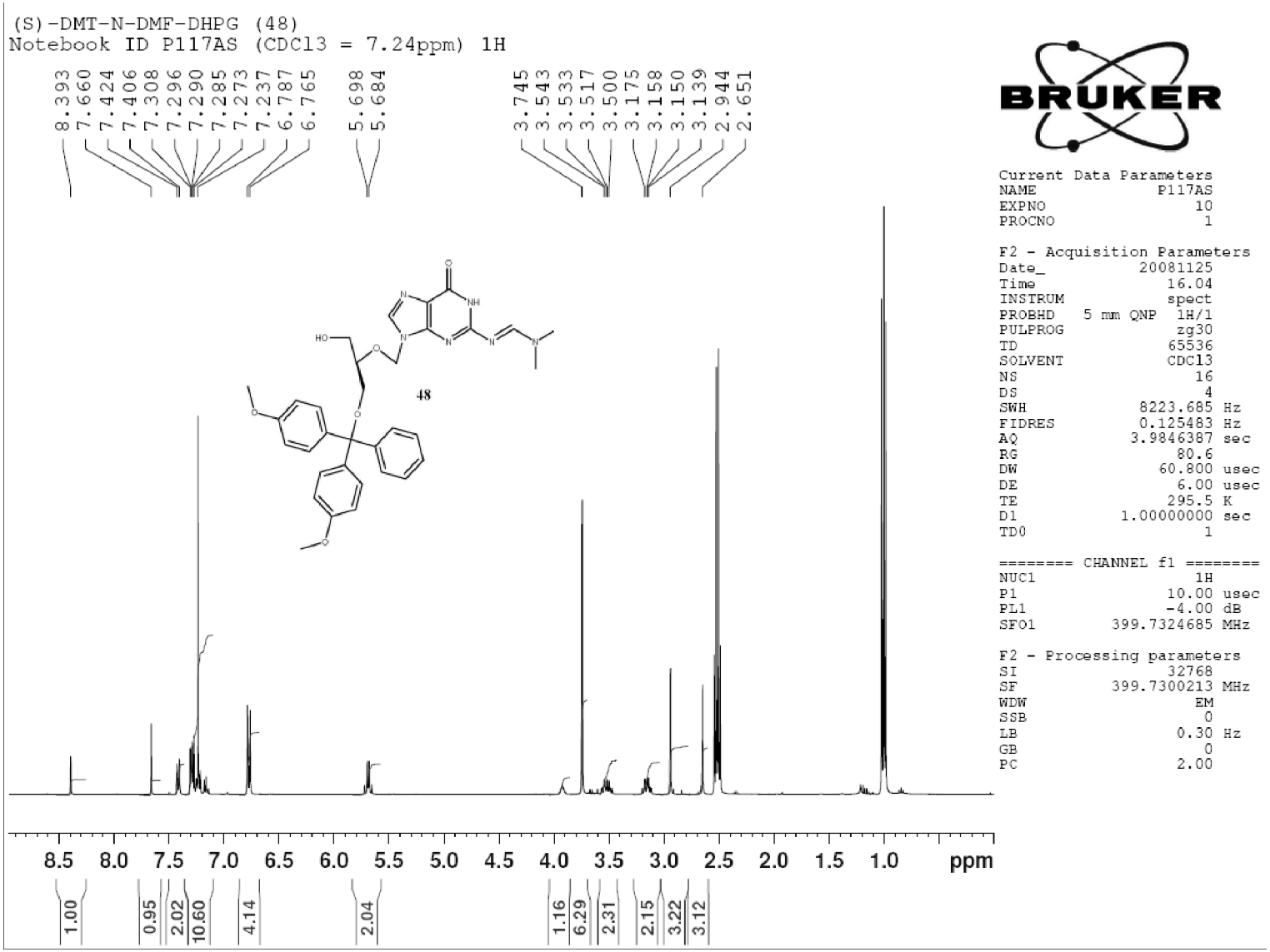

BRUKER

Current Data Parameters
NAME P117AS
EXPNO 10
PROCNO 1

F2 - Acquisition Parameters
Date_ 20081125
Time 16.04
INSTRUM spect
PROBHD 5 mm QNP 1H/1
PULPROG zg30
TD 65536
SOLVENT CDCl3
NS 16
DS 4
SWH 8223.685 Hz
FIDRES 0.125483 Hz
AQ 3.9846387 sec
RG 80.6
DW 60.800 usec
DE 6.00 usec
TE 295.5 K
D1 1.00000000 sec
TD0 1

======== CHANNEL f1 ========
NUC1 1H
P1 10.00 usec
PL1 -4.00 dB
SFO1 399.7324685 MHz

F2 - Processing parameters
SI 32768
SF 399.7300213 MHz
WDW EM
SSB 0
LB 0.30 Hz
GB 0
PC 2.00

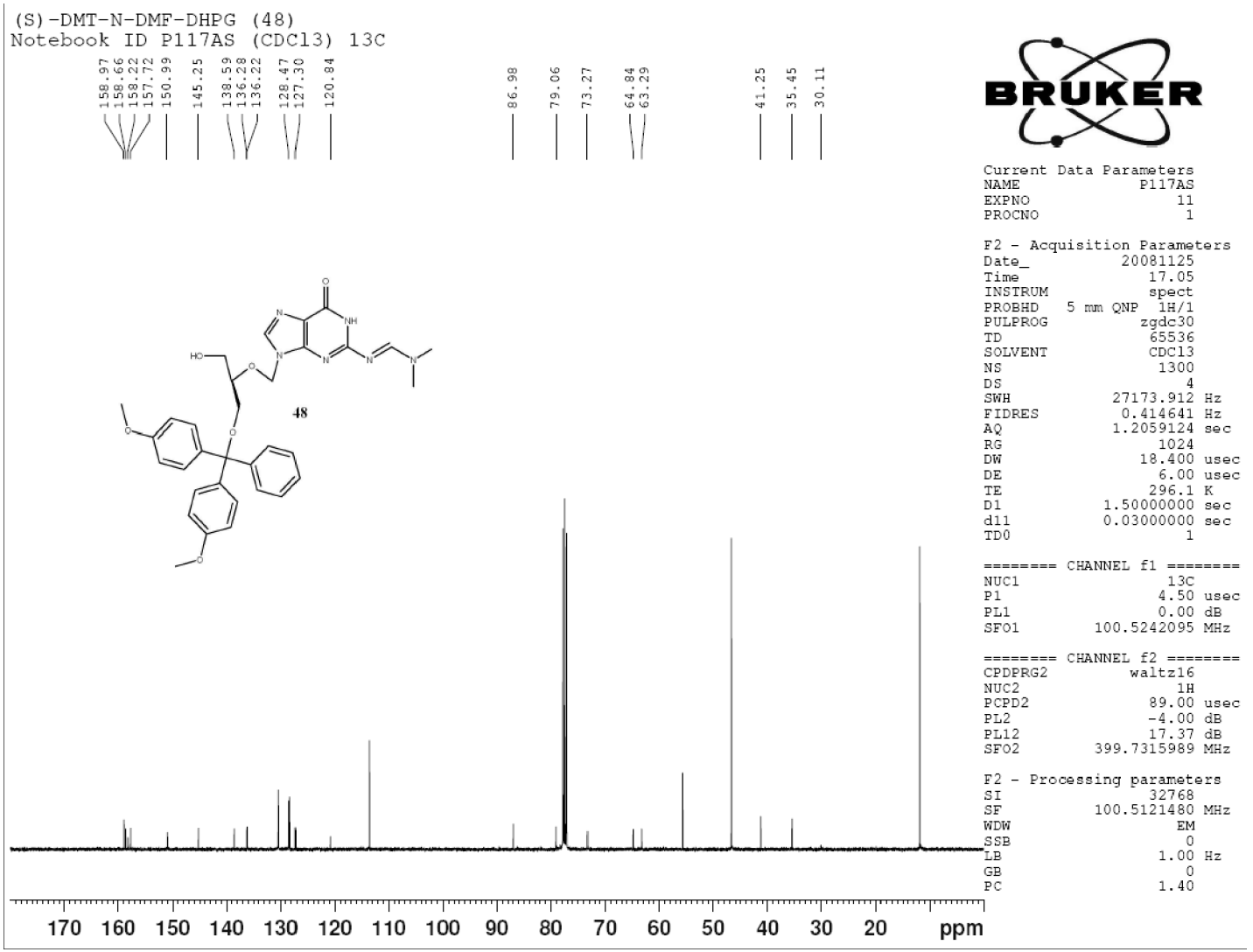
(S)-DMT-N-DMF-DHPG (48)
Notebook ID P117AS (CDCl3) 13C
158.97
158.66
158.22
157.72
150.99
145.25
138.59
136.28
136.22
128.47
127.30
120.84
86.98
79.06
73.27
64.84
63.29
41.25
35.45
30.11
48
170 160 150 140 130 120 110 100 90 80 70 60 50 40 30 20 ppm
Current Data Parameters
NAME P117AS
EXPNO 11
PROCNO 1
F2 - Acquisition Parameters
Date_ 20081125
Time 17.05
INSTRUM spect
PROBHD 5 mm QNP 1H/1
PULPROG zgdc30
TD 65536
SOLVENT CDC13
NS 1300
DS 4
SWH 27173.912 Hz
FIDRES 0.414641 Hz
AQ 1.2059124 sec
RG 1024
DW 18.400 usec
DE 6.00 usec
TE 296.1 K
D1 1.50000000 sec
d11 0.03000000 sec
TD0 1
======== CHANNEL f1 ========
NUC1 13C
P1 4.50 usec
PL1 0.00 dB
SFO1 100.5242095 MHz
======== CHANNEL f2 ========
CPDPRG2 waltz16
NUC2 1H
PCPD2 89.00 usec
PL2 -4.00 dB
PL12 17.37 dB
SFO2 399.7315989 MHz
F2 - Processing parameters
SI 32768
SF 100.5121480 MHz
WDW EM
SSB 0
LB 1.00 Hz
GB 0
PC 1.40

(S)-DMT-N-DMF-DHPG (48)
Notebook ID P117AS (D2O) DEPT135

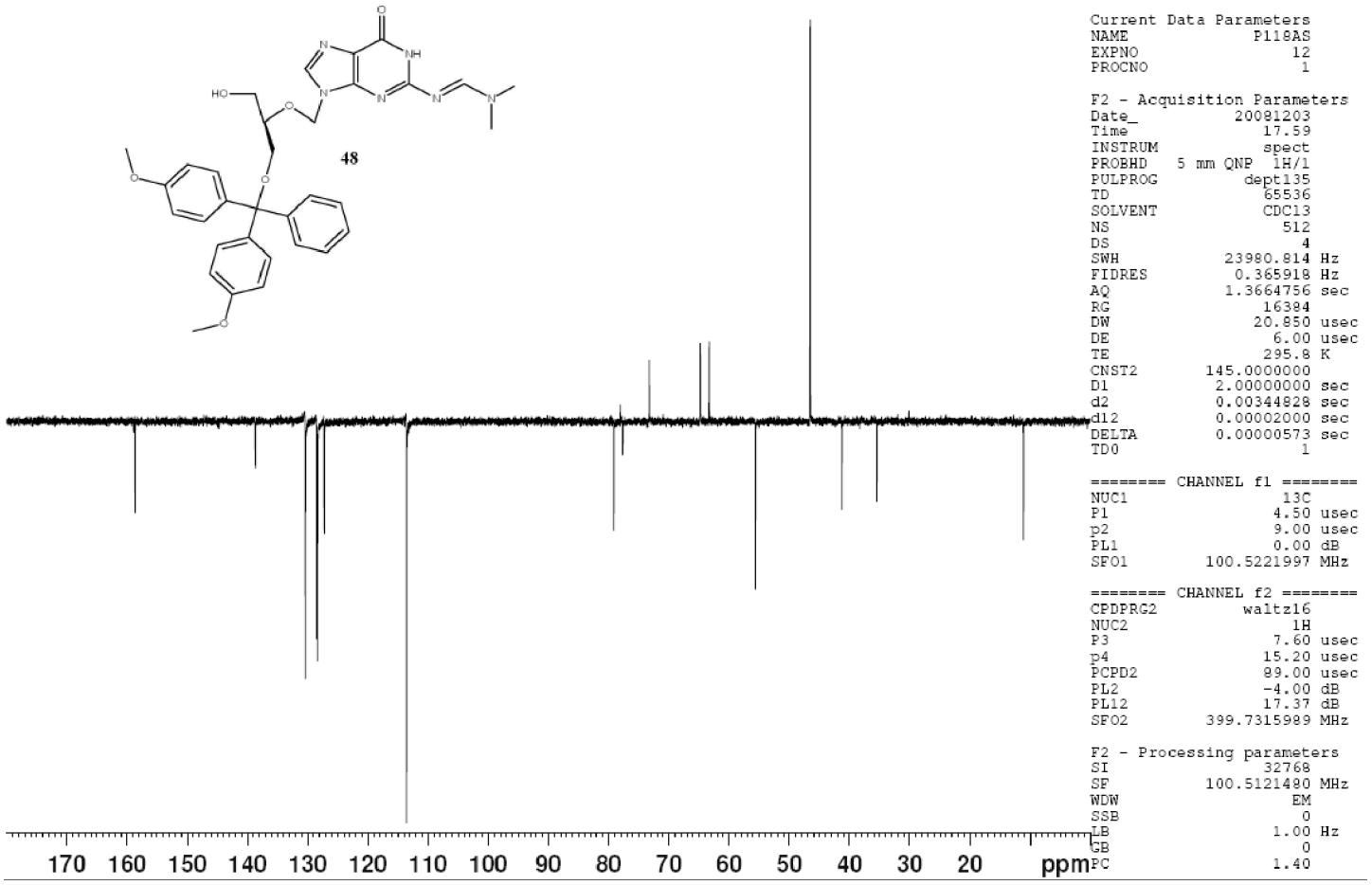

Current Data Parameters
NAME P118AS
EXPNO 12
PROCNO 1

F2 - Acquisition Parameters
Date_ 20081203
Time 17.59
INSTRUM spect
PROBHD 5 mm QNP 1H/1
PULPROG dept135
TD 65536
SOLVENT CDCl3
NS 512
DS 4
SWH 23980.814 Hz
FIDRES 0.365918 Hz
AQ 1.3664756 sec
RG 16384
DW 20.850 usec
DE 6.00 usec
TE 295.8 K
CNST2 145.0000000
D1 2.00000000 sec
d2 0.00344828 sec
d12 0.00002000 sec
DELTA 0.00000573 sec
TD0 1

======== CHANNEL f1 ========
NUC1 13C
P1 4.50 usec
p2 9.00 usec
PL1 0.00 dB
SFO1 100.5221997 MHz

======== CHANNEL f2 ========
CPDPRG2 waltz16
NUC2 1H
P3 7.60 usec
p4 15.20 usec
PCPD2 89.00 usec
PL2 -4.00 dB
PL12 17.37 dB
SFO2 399.7315989 MHz

F2 - Processing parameters
SI 32768
SF 100.5121480 MHz
WDW EM
SSB 0
LB 1.00 Hz
GB 0
PC 1.40

2,2′-anhydro-1-(B-D-arabinofuranosyl)uracil (58)
Notebook ID P124AS (D2O = 4.63) 1H

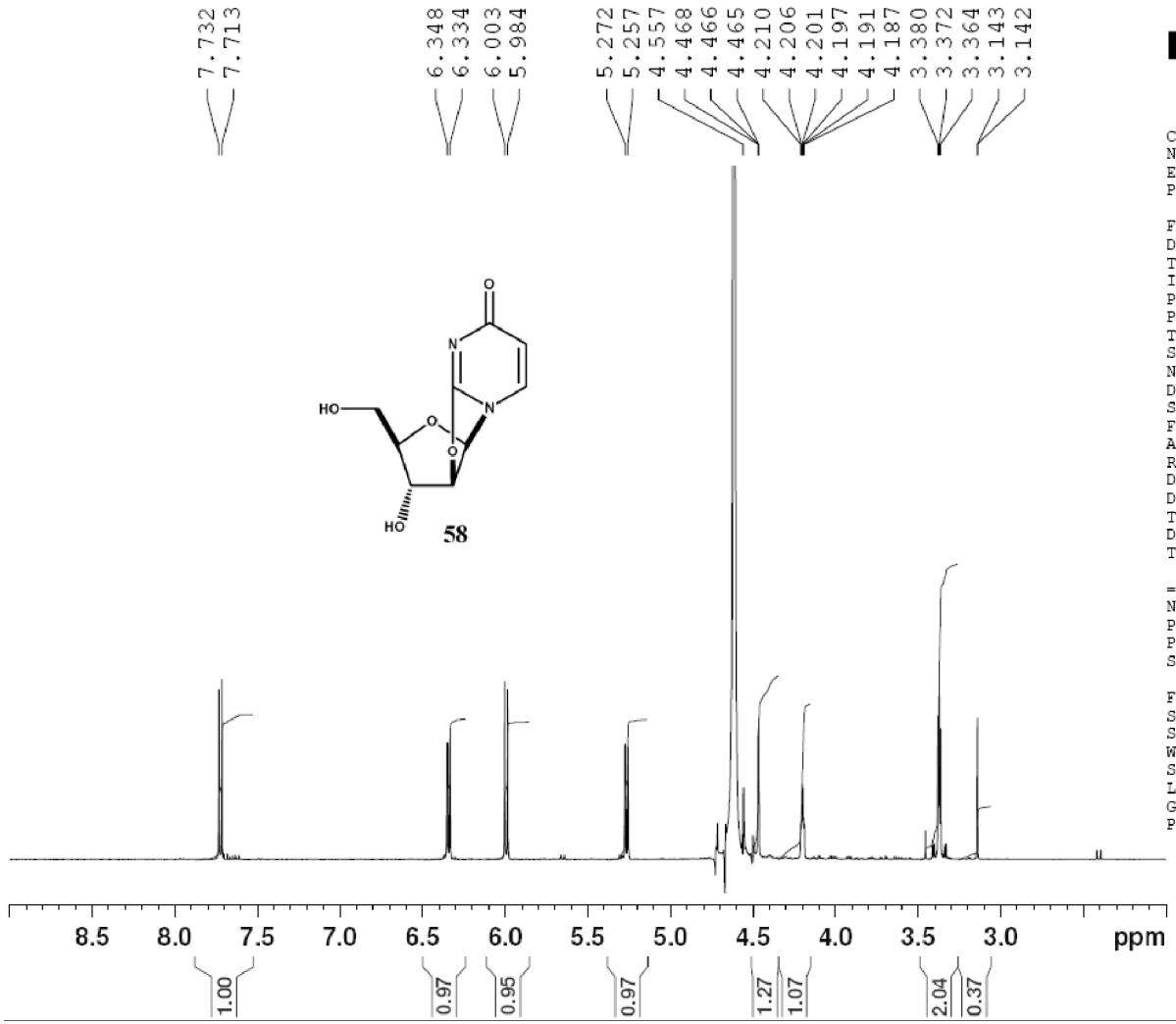

BRUKER

Current Data Parameters
NAME 58-shurer-0122
EXPNO 10
PROCNO 1

F2 - Acquisition Parameters
Date_ 20090123
Time 7.35
INSTRUM spect
PROBHD 5 mm QNP 1H/1
PULPROG zg30
TD 65536
SOLVENT D2O
NS 16
DS 4
SWH 8223.685 Hz
FIDRES 0.125483 Hz
AQ 3.9846387 sec
RG 80.6
DW 60.800 usec
DE 6.00 usec
TE 294.7 K
D1 1.00000000 sec
TD0 1

======== CHANNEL f1 ========
NUC1 1H
P1 10.00 usec
PL1 -4.00 dB
SFO1 399.7324685 MHz

F2 - Processing parameters
SI 32768
SF 399.7300368 MHz
WDW EM
SSB 0
LB 0.30 Hz
GB 0
PC 2.00

2,2′-anhydro-1-(B-D-arabinofuranosyl)uracil (58)
Notebook ID P124AS (D20) DEPT135

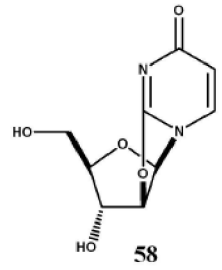

58

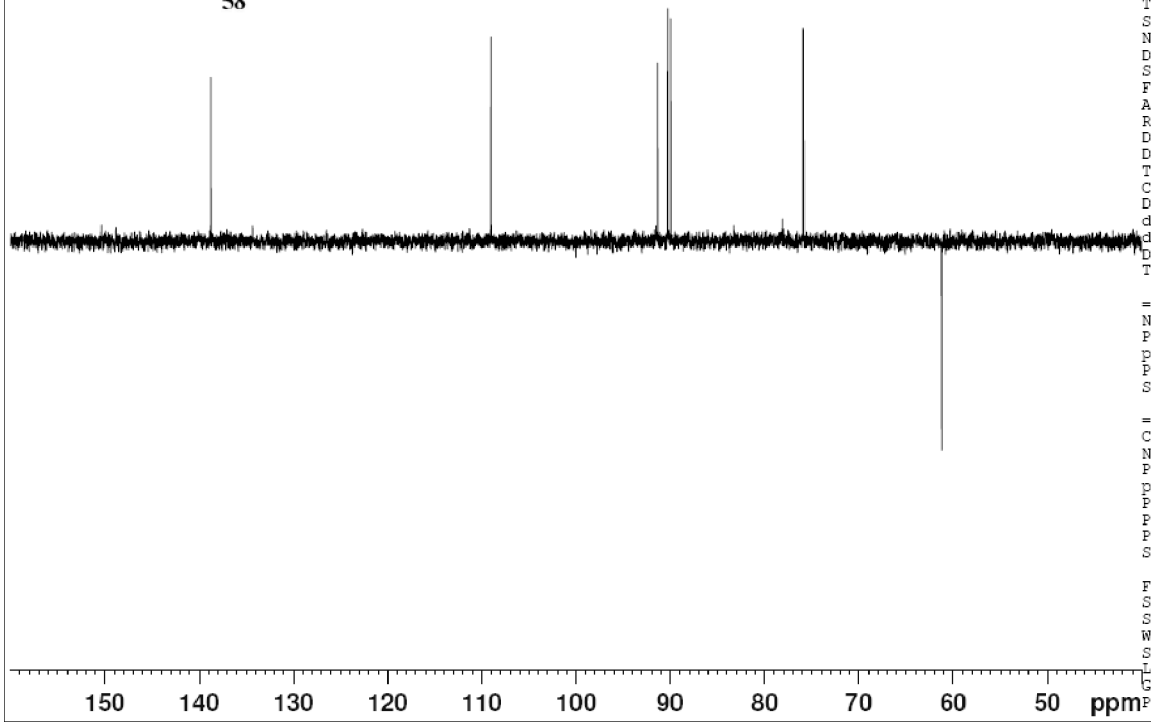

BRUKER

Current Data Parameters
NAME 58-shurer-0123
EXPNO 10
PROCNO 1

F2 - Acquisition Parameters
Date_ 20090123
Time 11.18
INSTRUM spect
PROBHD 5 mm QNP 1H/1
PULPROG dept135
TD 65536
SOLVENT D2O
NS 512
DS 4
SWH 23980.814 Hz
FIDRES 0.365918 Hz
AQ 1.3664756 sec
RG 16384
DW 20.850 usec
DE 6.00 usec
TE 295.1 K
CNST2 145.0000000
D1 2.00000000 sec
d2 0.00344828 sec
d12 0.00002000 sec
DELTA 0.00000573 sec
TD0 1

======== CHANNEL f1 ========
NUC1 13C
P1 4.50 usec
p2 9.00 usec
PL1 0.00 dB
SFO1 100.5221997 MHz

======== CHANNEL f2 ========
CPDPRG2 waltz16
NUC2 1H
P3 7.60 usec
p4 15.20 usec
PCPD2 89.00 usec
PL2 -4.00 dB
PL12 17.37 dB
SFO2 399.7315989 MHz

F2 - Processing parameters
SI 32768
SF 100.5121480 MHz
WDW EM
SSB 0
LB 1.00 Hz
GB 0
PC 1.40

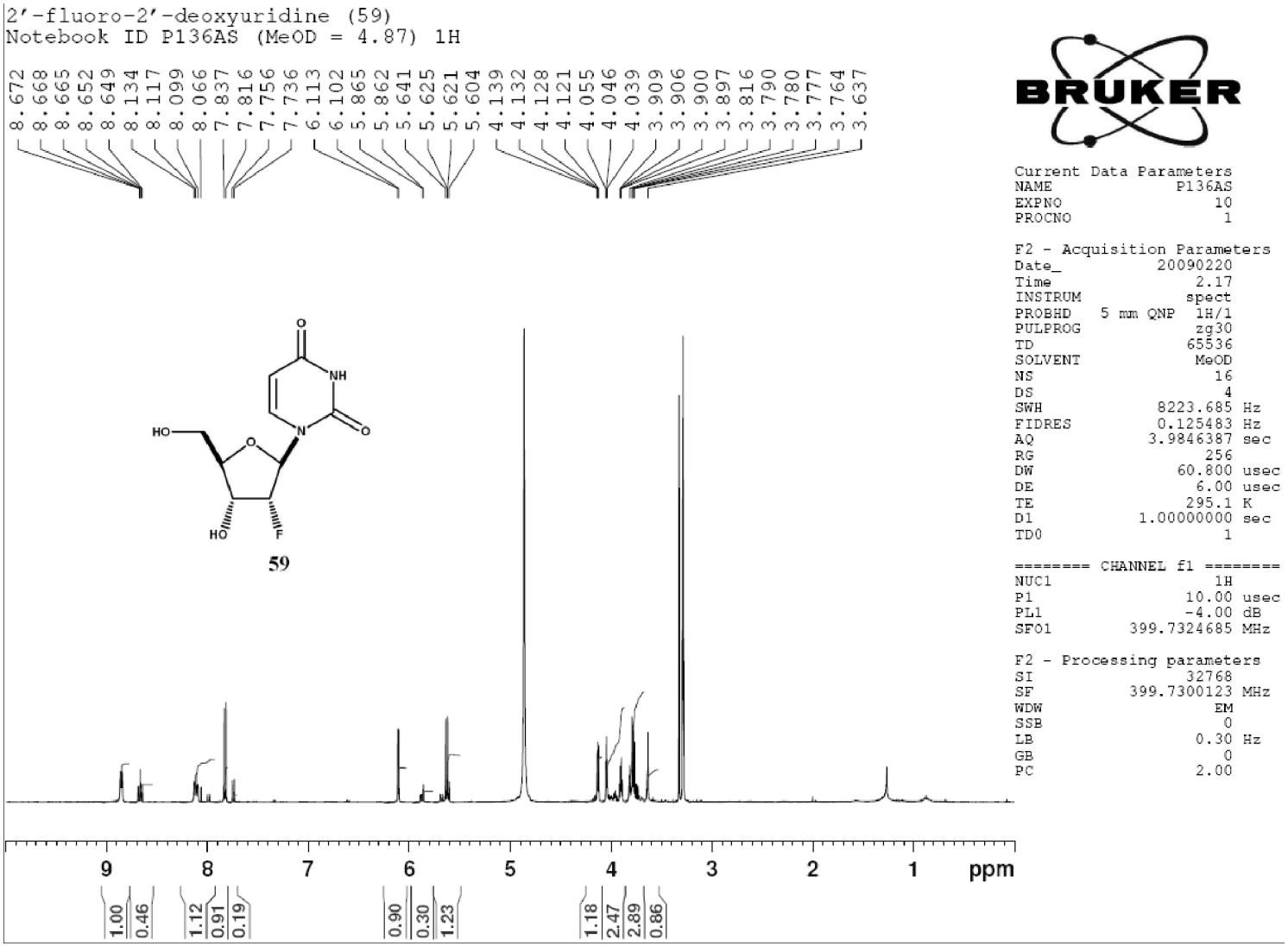
2′-fluoro-2′-deoxyuridine (59)
Notebook ID P136AS (MeOD = 4.87) 1H
8.672 8.668 8.665 8.652 8.649 8.134 8.117 8.099 8.066 7.837 7.816 7.756 7.736 6.113 6.102 5.865 5.862 5.641 5.625 5.621 5.604 4.139 4.132 4.128 4.121 4.055 4.046 4.039 3.909 3.906 3.900 3.897 3.816 3.790 3.780 3.777 3.764 3.637
HO
O
NH
N
O
HO
F
59
9 8 7 6 5 4 3 2 1 ppm
1.00 0.46 1.12 0.91 0.19 0.90 0.30 1.23 1.18 2.47 2.89 0.86
BRUKER
Current Data Parameters
NAME P136AS
EXPNO 10
PROCNO 1
F2 - Acquisition Parameters
Date_ 20090220
Time 2.17
INSTRUM spect
PROBHD 5 mm QNP 1H/1
PULPROG zg30
TD 65536
SOLVENT MeOD
NS 16
DS 4
SWH 8223.685 Hz
FIDRES 0.125483 Hz
AQ 3.9846387 sec
RG 256
DW 60.800 usec
DE 6.00 usec
TE 295.1 K
D1 1.00000000 sec
TD0 1
======== CHANNEL f1 ========
NUC1 1H
P1 10.00 usec
PL1 -4.00 dB
SFO1 399.7324685 MHz
F2 - Processing parameters
SI 32768
SF 399.7300123 MHz
WDW EM
SSB 0
LB 0.30 Hz
GB 0
PC 2.00

2′-fluoro-2′-deoxyuridine (59)
Notebook ID P136AS (MeOD) 19F

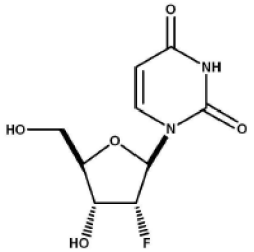

59


```
Current Data Parameters
NAME                  P136AS
EXPNO                     12
PROCNO                     1

F2 - Acquisition Parameters
Date_              20090220
Time                   3.24
INSTRUM               spect
PROBHD   5 mm QNP  1H/1
PULPROG                zg30
TD                    65536
SOLVENT                MeOD
NS                      128
DS                        4
SWH               45045.047 Hz
FIDRES             0.687333 Hz
AQ                0.7274996 sec
RG                   2580.3
DW                   11.100 usec
DE                     6.00 usec
TE                    295.1 K
D1             1.50000000 sec
TD0                       1

======== CHANNEL f1 ========
NUC1                    19F
P1                     8.00 usec
PL1                   -3.00 dB
SFO1           376.0770233 MHz

F2 - Processing parameters
SI                     32768
SF             376.1220284 MHz
WDW                       EM
SSB                        0
LB                      0.30 Hz
GB                         0
PC                      1.00
```

Bibliography

[1]Cohen, M. Changing patterns of infectious disease. *Nature.* **2000,** *406,* 762-767.

[2]Garrett, L. *AIDS in the World;* Mann, J.; Tarantola, D; Netter, T., Eds.; Harvard University Press: Cambridge, Massachusetts, 1992; pp 825–839.

[3]World Health Organization Report on Infectious Diseases: Removing Obstacles to Healthy Development. Geneva, Switzerland: World Health Organization; 1999.

[4]http://www.fda.gov/oc/opacom/hottopics/antiresist_facts.html (Accessed December, 2007).

[5]Nussbaum, F.; Brands, M.; Hinzen, B.; Weigand, S.; Häbich, D. Antibacterial Natural Products in Medicinal Chemistry - Exodus or Revival? *Angew. Chem., Int. Ed.* **2006,** *45,* 5072-5129.

[6]Culotta, E. Funding crunch hobbles antibiotic resistance research. *Science*, **1994,** *264,* 362–363.

[7]Bax, R. Antibiotic resistance: a view from the pharmaceutical industry. *Clin. Infect. Dis.,* **1997,** *24,* 5151–5153.

[8]Donlan, R.; Costerton, W. Biofilms: Survival Mechanisms of Clinically Relevant Microorganisms. *Clin. Microbiol. Rev.* **2002,** *15,* 167-193.

[9]Adams, J.; McLean, R. Impact of *rpoS* Deletion on *Escherichia coli* Biofilms. *Appl. Environ. Microbiol.* **1999,** *65,* 4285-4287.

[10]Tresse, O.; Jouenne, T.; Junter, G.; The role of oxygen limitation in the resistance of agar-entrapped, sessile-like *Escherichia coli* to aminoglycoside and ß-lactam antibiotics. *J. Antimicrob. Chemother.* **1995,** *36,* 521-526.

[11]Dagostino, L.; Goodman, A.; Marshall, K. Physiological responses induced in bacteria adhering to surfaces. *Biofouling.* **1991,** *4,* 113-119.

[12]Suci, P.; Mittelman, M.; Yu, F.; Geesey, G. Investigation of ciprofloxacin penetration into *Pseudomonas aeruginosa* biofilms. *Antimicrob. Agents Chemother.* **1994,** *38,* 2125-2133.

[13]Hoyle, B.; Wong, C.; Costerton, W. Disparate efficacy of tobramycin on Ca^{2+}-, Mg^{2+}-, and HEPES-treated *Pseudomonas aeruginosa* biofilms. *Can. J. Microbiol.* **1992,** *38,* 1214-1218.

[14]DuGuid, I.; Evans, E.; Brown, M.; Gilbert, P. Effect of biofilm culture upon the susceptibility of *Staphylococcus epidermidis* to tobramycin. *J. Antimicrob. Chemother.* **1992,** *30,* 803-810.

[15]Musk, D.; Hergendrother, P. Chemical Countermeasures for the Control of Bacterial Biofilms: Effective Compounds and Promising Targets. *Curr. Med. Chem.* **2006,** *13,* 2163-2177.

[16]Miller, M.; Bassler, B. Quorum Sensing in Bacteria. *Annu. Rev. Microbiol.* **2001,** *55,* 165-199.

[17]Romling, U.; Gomelsky, M.; Galperin, M. C-di-GMP: the dawning of a novel bacterial signalling system. *Mol. Microbiol.* **2005,** *57,* 629.

[18]Ross, P.; Weinhouse, H.; Aloni, Y.; Michaeli, D.; Ohana, P.; Mayer, R.; Braun, S.; de Vroom, E.; Van der Marel, G.; Van Boom, H.; Benziman, M. Regulation of cellulose synthesis in *Acetobacter xylinum* by cyclic di-guanylic acid. *Nature.* **1987,** *325,* 279-281.

[19]Berg, J.; Tymoczko, J.; Stryer, L. *Biochemistry;* W.H. Freeman and Company: New York, 2002; pp 382-383.

[20]Chang, A.; Tuckerman, J.; Gonzalez, G.; Mayer, R.; Weinhouse, H.; Volman, G.; Amikam, D.; Benziman, M.; Gilles-Gonzalez M. Phosphodiesterase A1, a regulator of cellulose synthesis in *Acetobacter xylinum,* is a heme-based sensor. *Biochemistry.* **2001,** 3420-3426.

[21]Sowden, L.; Colvin, J. Morphology, microstructure, and development of colonies of *Acetobacter xylinum*. *Can. J. Microbiol.* **1978,** *24,* 772-779.

[22]Cook, K.; Colvin, J. Evidence for a beneficial influence of cellulose production on growth of *Acetobacter xylinum* in liquid medium. *Curr. Microbiol.* **1980,** *3,* 203-205.

[23]Dow, J.; Fouhy, Y.; Lucey, J.; Ryan, R. The HD-GYP Domain, Cyclic Di-GMP Signaling, and Bacterial Virulence to Plants. *Molec. Plant-Microbe Int.* **2006,** *19,* 1378-1384.

[24]Chan, C.; Paul, R.; Samoray D.; Amiot, N.; Giese, B.; Jenal, U.; Schirmer, T. Structural basis of activity and allosteric control of diguanylate cyclase. *Proc. Natl. Acad. Sci. U.S.A.,* **2004,** *101,* 17084-17089.

[25]Tal, R.; Wong, H.; Calhoon, R.; Gelfand, D.; Fear, A.; Volman, G.; Mayer, R.; Ross, P.; Amikam, D.; Weinhouse, H.; Cohen, A.; Sapir, S.; Ohana, P.; Benziman, M. Three cdg Operons Control Cellular Turnover of Cyclic Di-GMP in *Acetobacter xylinum*: Genetic Organization and Occurrence of Conserved Domains in Isoenzymes. *J. Bacteriol.* **1998,** 4416-4425.

[26]Merkel, T.; Barros, C.; Stibitz, S. Characterization of the *bvgR* Locus of *Bordetella pertussis. J. Bacteriol.* **1998,** *180,* 1682-1690.

[27]Simm, R.; Morr, M.; Kadar, A.; Nimtz, M.; Romling, U. GGDEF and EAL domains inversely regulate cyclic di-GMP levels and transition from sessility to motility. *Mol. Microbiol.* **2004,** *53,* 1123-1134.

[28]Tischler, A.; Camilli, A. Cyclic diguanylate (c-di-GMP) regulates *Vibrio cholerae* biofilm formation. *Mol. Microbiol.* **2004,** *53,* 857-869.

[29]Tischler, A.; Camilli, A. Cyclic Diguanylate Regulates *Vibrio cholerae* Virulence Gene Expression. *Mol. Microbiol.* **2005,** *73,* 5873-5882.

[30]Hisert, K.; MacCoss, M.; Shiloh, M.; Darwin, K.; Singh, S.; Jones, R.; Ehrt, S.; Zhang, Z.; Gaffney, B.; Gandotra, S. A glutamate-alanine-leucine (EAL) domain protein of *Salmonella* controls bacterial survival in mice, antioxidant defence and killing of macrophages: role of cyclic diGMP. *Mol. Microbiol.* **2005,** *56,* 1234-1245.

[31]Liaw, Y.; Gao, Y.; Robinson, H.; Sheldrick, G.; Sliedregt, L.;Van der Marel, G.; Van Boom, J.; Wang, A. Cyclic Diguanylic Acid Behaves as a Host Molecule for Planar Intercalators. *FEBS Lett.* **1990,** *264,* 223-227.

[32]Guan, Y.; Gao, Y.; Liaw, Y.; Robinson, H.; Wang, A. Molecular structure of cyclic diguanylic acid at 1 A resolution of two crystal forms: self-association, interactions with metal ion/planar dyes and modeling studies. *J. Biomol. Struct. Dyn.* **1993,** *11,* 253-276.

[33]Zhang, Z.; Gaffney, B.; Jones, R. c-di-GMP Displays A Monovalent Metal Ion-Dependent Polymorphism. *J. Am. Chem. Soc.* **2004,** *126,* 16700-16701.

[34]Zhang, Z.; Kim, S.; Gaffney, B.; Jones, R. Polymorphism of the Signaling Molecule c-di-GMP. *J. Am. Chem. Soc.* **2006,** *128,* 7015-7024.

[35]De Vroom, E.; Fidder, A.; de Paus, P.; Sliedregt, L.; Van der Marel, G.; Van Boom, J. The cyclic diguanylic acid regulatory system of cellulose synthesis in *Acetobacter xylinum*. Chemical synthesis and biological activity of cyclic nucleotide dimer, trimer, and phosphothioate derivatives. *J. Biol. Chem.* **1990,** *265,* 18933-18943.

[36]Hayakawa, Y.; Nagora, R.; Hirata, A.; Hyodo, M.; Kawai, R. A facile synthesis of cyclic bis(3'-5')diguanylic acid. *Tetrahedron,* **2003,** *59*, 6465-6471.

[37]Gasparutto, D.; Livache, T.; Bazin, H.; Duplaa, A.; Guy, A.; Khorlin, A.; Molko, D.; Roget, A.; Teoule, R. Chemical synthesis of a biologically active natural tRNA with its minor bases. *Nucleic Acids Res.* **1992,** *20,* 5159-5166.

[38]Conte, M.; Mayol, L.; Montesarchio, D.; Piccialli, G.; Santacroce, C. Automated Synthesis of Cyclic Oligodeoxyribonucleotides via Phosphoramidite Method. *Nucleosides Nucleotides.* **1993,** *12,* 351-358.

[39]DeNapoli, L.; Galeone, A.; Mayol, L.; Messere, A.; Piccialli, G.; Santacroce, C. Facile preparation of cyclic oligoribonucleotides. *J. Chem. Soc. Perkin. Trans.* **1993,** 747-749.

[40]Alazzouzi, E.; Escaja, N.; Grandas, A.; Pedroso, E. A Straightforward Solid-Phase Synthesis of Cyclic Oligodeoxyribonucleotides. *Angew. Chem., Int. Ed*. **1997,** *36,* 1506-1508.

[41]Smietana, M.; Kool, E. Efficient and Simple Solid-Phase Synthesis of Short Cyclic Oligodeoxynucleotides Bearing a Phosphorothioate Linkage. *Angew. Chem., Int. Ed.* **2002,** *41,* 3704-3707.

[42]Kiburu, I.; Shurer, A.; Yan, L.; Sintim, H. A simple solid-phase synthesis of the ubiquitous bacterial signaling molecule, c-di-GMP and analogues. *Mol. BioSyst.,* **2008,** *4,* 518–520.

[43]Chan, C.; Paul, R.; Samoray, D.; Amiot, N.; Giese, B.; Jenal, U.; Schirmer, T. Structural basis of activity and allosteric control of diguanylate cyclases. *Proc. Natl. Acad. Sci. U.S.A.* **2004,** *101,* 17084-17089.

[44]Bloomfield, V.; Crothers, D.; Tinoco, I. *Nucleic Acids;* University Science Books: California, 1999; pp 18-19.

[45]Patnaik, S.; Kumar, P.; Garg, B.; Gandhi, R.; Gupta, K. Photomodulation of PS-modified oligonucleotides containing azobenzene substituent at pre-selected positions in phosphate backbone. *Bioorg. Med. Chem.* **2007,** *15,* 7840-7849.

[46]Xie, C.; Staszak, M.; Quatroche, J.; Sturgill, C.; Khau, V.; Martinelli, M. Nucleosidic Phosphoramidite Synthesis via Phosphitylation: Activator Selection and Process Development. *Org. Process. Res. Dev.* **2005,** *9,* 730-737.

[47]Marshalko, S.; Schweitzer, B.; Beardsley, G. Chiral Chemical Synthesis of DNA Containing (S)-9-(1,3-Dihydroxy-2-propoxymethyl)guanine (DHPG) and Effects on Thermal Stability, Duplex Structure, and Thermodynamics of Duplex Formation. *Biochemistry.* **1995,** *34,* 9235-9248.

[48]Mourani, R.; Damha, M. Synthesis, Characterization, and Biological Properties of Small Branched RNA Fragments Containing Chiral (R_P and S_P) 2'-5'-Phosphorotioate Linkages. *Nucleosides Nucleotides Nucleic Acids.* **2006,** *25,* 203-229.

[49]Zaiseva, G.; Zinchenko, A.; Barai, V.; Pavlova, N.; Boreko, E.; Mikhaiopulo, I. Chemical and Enzymatic Synthesis and Antiviral Properties of 2'-Deoxy-2'-fluoroguanosine. *Nucleosides Nucleotides.* **1999,** *18,* 687-688.

[50]Mikhailopulo, I.; Poopeiko, N.; Sivets, G.; Khripach, N. Oxidation-reduction sequence for the synthesis of peracylated fluorodeoxy pentofuranosides. *Carbohyd. Res.* **1995,** *278,* 71-89.

[51]Verheyden, J.; Wagner, D.; Moffatt, J. Synthesis of Some Pyrimidine 2'-Amino-2'-deoxynucleosides. *J. Org. Chem*. **1971,** *36,* 250-254.

[52]Dai, Q.; Deb, S.; Hougland, J.; Piccirilli, J. Improved synthesis of 20-amino-20-deoxyguanosine and its phosphoramidite. *Bioorg. Med. Chem.* **2006,** *14,* 705-713.

[53]Bloomfield, V.; Crothers, D.; Tinoco, I. *Nucleic Acids;* University Science Books: California, 1999; pp 50-51.

[54]Saito, Y.; Matsumoto, K.; Bag, S.; Ogasawara, S.; Fujimoto, K.; Hanawa, K.; Saito, I. C8-alkynyl- and alkylamino substituted 20-deoxyguanosines: a universal linker for nucleic acids modification. *Tetrahedron*. **2008,** *64,* 3578-3588.